Global Environmental Change 39 (2016) 108–124

Contents lists available at ScienceDirect

Global Environmental Change

journal homepage: www.elsevier.com/locate/gloenvcha

Mapping global patterns of drought risk: An empirical framework based on sub-national estimates of hazard, exposure and vulnerability☆

Hugo Carrão *, Gustavo Naumann, Paulo Barbosa

European Commission (EC), Joint Research Centre (JRC), Via Enrico Fermi 2749, 21027 Ispra, VA, Italy

ARTICLE INFO

Article history:
Received 30 October 2015
Received in revised form 24 February 2016
Accepted 26 April 2016
Available online 18 May 2016

Keywords:
Drought risk management
Non-parametric composite indicators
Global
Hazard
Exposure
Vulnerability

ABSTRACT

A global map of drought risk has been elaborated at the sub-national administrative level. The motivation for this study is the observation that little research and no concerted efforts have been made at the global level to provide a consistent and equitable drought risk management framework for multiple regions, population groups and economic sectors. Drought risk is assessed for the period 2000–2014 and is based on the product of three independent determinants: hazard, exposure and vulnerability. Drought hazard is derived from a non-parametric analysis of historical precipitation deficits at the 0.5°; drought exposure is based on a non-parametric aggregation of gridded indicators of population and livestock densities, crop cover and water stress; and drought vulnerability is computed as the arithmetic composite of high level factors of social, economic and infrastructural indicators, collected at both the national and sub-national levels. The performance evaluation of the proposed models underlines their statistical robustness and emphasizes an empirical resemblance between the geographic patterns of potential drought impacts and previous results presented in the literature. Our findings support the idea that drought risk is driven by an exponential growth of regional exposure, while hazard and vulnerability exhibit a weaker relationship with the geographic distribution of risk values. Drought risk is lower for remote regions, such as tundras and tropical forests, and higher for populated areas and regions extensively exploited for crop production and livestock farming, such as South-Central Asia, Southeast of South America, Central Europe and Southeast of the United States. As climate change projections foresee an increase of drought frequency and intensity for these regions, then there is an aggravated risk for global food security and potential for civil conflict in the medium- to long-term. Since most agricultural regions show high infrastructural vulnerability to drought, then regional adaptation to climate change may begin through implementing and fostering the widespread use of irrigation and rainwater harvesting systems. In this context, reduction in drought risk may also benefit from diversifying regional economies on different sectors of activity and reducing the dependence of their GDP on agriculture.

1. Introduction

Few recurring and extreme natural events are as environmental, economic and socially disruptive as droughts, which affect millions of people in the world each year (Wilhite, 2000; Cooley, 2006). Although droughts are typically associated with aridity (Seager et al., 2007; Güneralp et al., 2015), they can virtually occur over most parts of the world, even in wet and humid regions, and can profoundly impact on agriculture, basic household welfare, tourism, ecosystems and the services they provide (Goddard et al., 2003; Dai, 2011). Recent disasters in developing and developed countries and the concomitant impacts and personal hardships

☆ This research received support from the EUROCLIMA regional cooperation program between the European Union (European Commission; DG DEVCO) and Latin America. Research by Gustavo Naumann was funded by the European Union Seventh Framework Programme FP7/2007-2013 under grant agreement no. 603864 (HELIX: High-End cLimate Impacts and eXtremes). The authors thank the two anonymous reviewers for their comments and suggestions that served to clarify a number of points and to greatly improve the original version of the manuscript.

* Corresponding author.
E-mail addresses: hugo.carrao@gmail.com (H. Carrão), paulo.barbosa@jrc.ec.europa.eu (P. Barbosa).

http://dx.doi.org/10.1016/j.gloenvcha.2016.04.012

that resulted have underscored the exposure and vulnerability of all societies to this natural hazard (Wilhite et al., 2007; Mishra and Singh, 2009). However, drought management in most parts of the world is still reactive, responding to drought after impacts have occurred (Hayes et al., 2004; Svoboda et al., 2015; Wilhite et al., 2007, 2014). This approach – commonly referred to as crisis management – is known to be untimely, poorly coordinated and disintegrated (Wilhite and Pulwarty, 2005). Moreover, the provision of drought relief or assistance to those most affected has been shown to decrease socioeconomic capabilities to face future drought episodes by reducing self-reliance and increasing dependence on government and donor organizations (Wilhite et al., 2014; Pulwarty and Sivakumar, 2014).

As a result, past attempts to manage drought disasters have been ineffective and its economic and social impacts have increased significantly worldwide (Peterson et al., 2013; Sivakumar et al., 2014). Indeed, because of their long-lasting socioeconomic impacts, droughts are by far considered the most damaging of all natural disasters (Sivakumar et al., 2014). Over the United States, droughts cause $6–8 billion per year damages on average, but as much as 22 events between 1980 and 2014 resulted in over $200 billion costs (NCDC, 2015). Current estimates by the European Commission (CEC, 2007) indicate that the damages of droughts in Europe over the last 30 years are at least €100 billion. On top of that, the European Environmental Agency EEA (2010) reported that the annual average economic impact from droughts doubled between 1976–1990 and 1991–2006, rising to €6.2 billion per year in the most recent period. In India a drought has been reported at least once in every three years in the last five decades (Mishra et al., 2009; UNISDR, 2009a). Moreover, the country has suffered a financial loss of about $149 billion and 350 million people got affected due to droughts in the past 10 years (Gupta et al., 2011).

While large economic impacts of droughts are most relevant in wealthy industrialized nations, its social impacts are particularly severe in food-deficit countries with high dependence on subsistence agriculture and primary sector activities (Reed, 1997). In such cases, drought events combined with poor governance and poorly functioning market systems, oppressive policies, and intermittent or insufficient food aid, has historically lead to food insecurity, famine, human conflicts and widespread mortality (Below et al., 2007; Gráda, 2007). For example, severe droughts in the 1980s resulted in massive socioeconomic disruptions in the West African Sahel: pastures and water bodies were largely depleted, local populations suffered severe food shortages, and over half a million people were killed (Hulme, 1996; Kallis, 2008; Traore et al., 2014). In North Africa, four severe droughts between 2000 and 2011 brought 2–3 million people in extreme poverty and wiped out 80–85% of herd stock (UN-DESA, 2013). More recently, some analysts have argued that disasters related to drought, including agriculture failing, water shortages and water mismanagement have played an important role in contributing to the deterioration of social structures and spurring violence that began in Syria in March 2011 (Gleick, 2014; Kelley et al., 2015).

In order to reduce the global threat of drought, an increasing number of international initiatives, such as the "Hygo Framework for Action 2005–2015: Building resilience of Nations and Communities to Disaster" (UNISDR, 2009a,b) and the "High-level Meeting on National Drought Policy" (WMO, 2013), have begun to encourage all the governments around the world to move towards a drought-resilient society. Although providing a safety net for those people or sectors most vulnerable to drought is always a high priority, the challenge now is to do it in a manner that engenders cooperation and coordination between different levels of governance in order to reinforce the tenets of proactive drought risk reduction strategies (Kampragou et al., 2011; Sivakumar et al., 2014; Wilhite et al., 2014). This new paradigm emphasizes greater understanding of both the natural features of drought and the factors that influence social and economic vulnerability. In this context, progress on global drought risk management is particularly important. It addresses questions that are difficult (or currently impossible) for local management to address, namely those related to tightly interlocked global impacts that cause and/or exacerbate local economic and social vulnerability, such as increasing food prices and food insecurity (Dai, 2011; Pozzi et al., 2013; Wilhite et al., 2014). If food prices continue to increase, it will seriously compromise efforts to reduce vulnerability and regions with increasing food insecurity will be progressively less adapted to drought hazard (UNISDR, 2009b). Since international support on risk management to those most affected is based on prioritized adaptive needs, and regional cooperation funds to reinforce national adaptation plans are most reflected in decisions taken at the global level, then it is extremely important to identify the regions where drought impacts might be especially sensitive and development aid can be best concentrated (Alcamo and Henrichs, 2002; UNISDR, 2009b).

Despite current concerns about increasing drought impacts on food, water and energy sectors, several authors have warned that more global efforts are spent on studying and quantifying drought as a natural hazard than at providing a consistent and equitable drought risk management framework for multiple regions, population groups and economic sectors (Eriyagama et al., 2009; Kampragou et al., 2011; Shiau and Hsiao, 2012; Pulwarty and Sivakumar, 2014; Kim et al., 2015; González Tánago et al., 2015). In this paper we, therefore, provide practical insight into useful and freely available science-based resources for mapping the global patterns of drought risk. We concentrate on a data-driven approach that is based on the combination of independent indicators of historical drought hazard and current estimates of drought exposure and vulnerability, as previously suggested by Dao and Peduzzi (2003), Peduzzi et al. (2009) and Cardona et al. (2012). It is a kind of first screening analysis to determine where local assessments should be carried out to improve adaptation plans and mitigation activities, and strengthen multiscale drought risk management policies. Moreover, comparing risk across regions can identify leverage points in reducing impacts from drought and, by inference, from climate change, which is likely to be manifested through increases in the frequency of drought events at least in the short- to medium-term. The paper is organized as follows: this section begins by examining the underlying concepts of drought impacts, crisis and risk management; Section 2 gives an overview of drought risk and the proposed efforts for estimating its determinants; in the third section, the data used for mapping the global distribution of drought risk and its determinants are described, and the performance assessment to evaluate the robustness of the underlying models is outlined; after a discussion about the spatial distribution of risk and its determinants in Section 4, the study is concluded in Section 5.

2. Defining and mapping drought risk

Definitions of risk are commonly probabilistic in nature, referring to the potential losses from a particular hazard to a specified element at risk in a particular future time period (Blaikie et al., 1994; Brooks et al., 2005). Drought risk is the probability of harmful consequences or likelihood of losses resulting from interactions between drought hazard (i.e. the possible future occurrence of drought events), drought exposure (i.e. the total population, its livelihoods and assets in an area in which drought events may occur), and drought vulnerability (i.e. the propensity of exposed elements to suffer adverse effects when impacted by a drought event) (Cardona et al., 2012). Expressed in another way, risk is determined not only by the amount of exposed entities and physical intensity of the natural hazard, but also by the vulnerability of society at a given moment in time – vulnerability is dynamic in response to changes in the economic, social, and infrastructural characteristics of the locale or region (Wilhite et al., 2007). There are three determinants of drought risk, whose relations we find it convenient to schematize in a mathematical form, as defined by Dao and Peduzzi (2003), Peduzzi et al. (2009) and Cardona et al. (2012):

$$\text{Risk} = \text{Hazard} \times \text{Exposure} \times \text{Vulnerability} \tag{1}$$

Since mitigation and preparedness plans conceiving more drought resilient ecosystems are engendered by national policies, and recovery aid from drought impacts tends to be distributed to government authorities in the first place, then we propose to compute Eq. (1) at the sub-national administrative level. This mapping unit provides decision makers and stakeholders with effective, standardized and systematic means for assessing drought impacts within political jurisdictions, and allows for better coordination and collaboration within and between different levels of government (Brooks et al., 2005; Wilhite et al., 2014).

The scores of regional drought risk range on a scale of 0–1, where 0 represents the lowest risk and 1 is associated with the highest risk. Because of the conceptual product relationship presented in Eq. (1), if there is no chance for the hazard or there is no exposure, then the risk for that location is null (Hayes et al., 2004). Therefore, in order to include the determinants of risk in the model, we need also to normalize them on the range between 0 and 1, which scores are associated, respectively, with the lowest and highest hazard, exposure and vulnerability conditions. As similar as for the Human Development Index (HDI) (UNDP, 2013), the Drought Vulnerability Index (DVI) (Naumann et al., 2014) and the Multidimensional Poverty Index (MPI) (Alkire and Santos, 2014), to cite but a few, the normalization takes into account the maximum and minimum values of each determinant across all available sub-national administrative regions. Thus, the model of drought risk is relative to the sample of geographic regions used to normalize the determinants of risk and their statistical distributions. The proposed scale of risk is not a measure of absolute losses or actual damage to human health or the environment, but suitable for ranking and comparison of input regions, as similar to the HDI (UNDP, 2013) and the MPI (Alkire and Santos, 2014). Another entry point for both understanding and addressing the potential losses of drought disasters is to simply measure the absolute magnitude of the exposed elements at a region (Brooks et al., 2005). Probabilistic (risk-based) and absolute (exposure-based) metrics represent alternative but complementary ways of approaching drought losses at different coordination levels. Quantitative measures are most important for local management when preparedness plans and mitigation activities are put in practice.

The drought risk model focus on the period 2000–2014. A time span considering the most recent 15 years was chosen for guarantying a global homogeneous level of information quality and completeness. This process is analogous to that proposed by Peduzzi et al. (2009), which focused on a 26-year period, from 1980 to 2006, for computing an updated global Disaster Risk Index.

2.1. Modeling drought hazard

Hazard refers to the natural or human induced events that potentially damage different places singly or in combination (Blaikie et al., 1994). In technical settings, hazards are described quantitatively by the frequency of events occurring at different intensities for different areas, as determined from historical data or scientific analysis (Reed, 1997; UNISDR, 2009a). Drought differs from other hazard types in several ways. First, unlike earthquakes, floods or tsunamis that occur along generally well-defined fault lines, river valleys or coastlines, drought can occur anywhere (with the exception of desert regions where it does not have meaning) (Goddard et al., 2003; Dai, 2011). Secondly, drought develops slowly, resulting from a prolonged period (from months to years) of precipitation that is below the average, or expected, value at a particular location (Dracup and Lee, 1980; Wilhite and Glantz, 1985).

These characteristics of drought make it particularly challenging to distinguish between hazard and disaster. In the literature, hazard usually refers to the natural phenomenon of a drought and the term disaster to its negative human and/or environmental impacts (e.g. Dracup and Lee, 1980; Wilhite and Glantz, 1985; Heim, 2002; Keyantash and Dracup, 2002; Mishra and Singh, 2009; Svoboda et al., 2012; Van Loon and Van Lanen, 2013). Following the distinction between hazard and disaster, those authors agree that all types of drought originate from a deficiency of precipitation, and that agricultural, hydrological, and socioeconomic droughts may be considered a follow-up of the meteorological drought. This classification highlights the interaction or interplay between the natural characteristics of the meteorological event (duration and magnitude of precipitation deficits) and the human activities that depend on precipitation to provide adequate water supplies to meet numerous social demands (Wilhite et al., 2007). Therefore, drought, as a natural hazard, results from an extreme deficiency of precipitation as compared to the expected climate "normal"; when extended over a season or longer, precipitation deficits might be insufficient to fulfill the requirements of an economic good or service and cause agricultural, hydrological and/or socioeconomic disasters (Dracup and Lee, 1980; Wilhite and Glantz, 1985; Heim, 2002; Wilhite and Buchanan, 2005).

Since precipitation is a proxy indicator of the water available to the coupled human–environment system (Svoboda et al., 2012), then the frequency of abnormal precipitation deficits at some level of intensity can be used to represent drought hazard for drought-prone nations and regions, as similar as proposed by Shahid and Behrawan (2008), He et al. (2012), Shiau and Hsiao (2012), and Kim et al. (2015), to cite but a few. In this study, drought hazard (dh) for region i is estimated as the probability of exceedance the median of global severe precipitation deficits for an historical reference period of N years, as follows:

$$dh_i = 1 - Pr\{S_i \leq \tilde{S}\} \tag{2}$$

where S_i represents the sorted set of severity values for all historical precipitation deficits at region i, and $\tilde{S}$ denotes the 50th percentile of global severe precipitation deficits. The severity of each precipitation deficit is computed by means of the weighted anomaly of standardized precipitation (WASP) index (Lyon and Barnston, 2005). The reasons for selecting the WASP-index are threefold: (1) it is standardized in time and space; (2) allows to damp large standardized anomalies that result from small precipitation amounts occurring near the beginning or end of dry seasons; and (3) emphasizes anomalies during the heart of rainy seasons (Andrade and Belo-Pereira, 2015). The WASP-index takes into account the annual seasonality of precipitation cycle and is computed by summing weighted standardized monthly precipitation anomalies, as follows (Lyon and Barnston, 2005):

$$s_j = \text{WASP}_j = \sum_{P_{n,m} < \tau_m}^{P_{n,m} \geq \tau_m} \left(\frac{P_{n,m} - \tau_m}{\tau_m} \right) \frac{\tau_m}{\tau_A}, \tag{3}$$

where τ_m, $1 \leq m \leq 12$, defines the monthly threshold of meteorological drought onset, and $\tau_A = \sum_{m=1}^{12} \tau_m$ is the maximum annual precipitation deficit due to drought conditions. A drought event j starts at year n and month m if $P_{n,m} < \tau_m$, and ends when $P_{n,m} \geq \tau_m$. τ_m is computed from a time-series of precipitation totals, $P_{m,1}, \ldots, P_{m,N}$, collected for the historical period of N years. The thresholds of drought onset are derived by means of the "Fisher–Jenks" classification algorithm, which estimates the monthly precipitation values that optimize the partition of the time-series into "drought" and "non-drought" months, as described in Carrão et al. (2014).

2.2. Inventorying drought exposure

To assess the impacts of drought hazard, the first step is to inventory and analyze the environment that can be damage (Di Mauro, 2014). In general, exposure data identifies the different types of physical entities that are on the ground, including built assets, infrastructures, agricultural land and people, to cite but a few (Peduzzi et al., 2009). As a slow onset hazard, drought exposure is very different from that of sudden hazards, such as earthquakes or storms. Although many droughts lead to severe economic and social impacts, few droughts show recorded mortality in international disaster databases (Peduzzi et al., 2009). Those that do cause mortality have generally occurred during a political crisis or civil conflict where aid could not reach the affected population (Gráda, 2007). Therefore, since available impact datasets do not provide information on the factors contributing directly to human casualties, then mortality is not a good proxy of drought exposure (UNISDR, 2009a,b).

Nevertheless, to overcome the difficulties associated with identifying, standardizing and combining the amounts of different elements at risk in the same geographic region, previous work has only focused on socioeconomic indicators and considered univariate standardized losses of human casualties as a proxy to drought exposure (e.g. Brooks et al., 2005; Peduzzi et al., 2009). To address this limitation, this paper proposes a non-compensatory model of drought exposure (de_i) to estimate the potential losses from different types of drought disasters at each geographic region i. The approach to drought exposure is comprehensive and takes into account the spatial distribution of population and the amount of numerous physical elements (proxy indicators) characterizing agriculture and primary sector activities, namely: crop areas (agricultural drought), livestock (agricultural drought), industrial/domestic water stress (hydrological drought), and human population (socioeconomic drought). In a non-compensatory model, the superiority in one indicator cannot be offset by an inferiority in some other indicator(s). Thus, a region is highly exposed to drought if at least one type of assets is abundant there. For example, an agricultural region that is completely covered by rainfed crops is fully exposed to drought, independently of the presence of other elements at risk.

Among different non-compensatory methods, Data Envelopment Analysis (DEA) (Lovell and Pastor, 1999; Cook et al., 2014) is a deterministic and non-parametric linear programming technique that can be used to quantify the relative exposure of a region to drought from a multidimensional set of indicators. DEA has widely and successfully been employed to measure the relative socioeconomic welfare of countries and their global rankings (Anderson et al., 2011), as well as to empirically categorize human development based on indicators of well-being and life satisfaction (Ramos and Silber, 2005). In addition, DEA can be used to monitor drought exposure through time, as similar as for comparing the inter-annual efficiency of health systems between countries from a time-series of cross-sectional multivariate indicators (Gupta and Verhoeven, 2001).

In the DEA methodology, the relative exposure of each region to drought is determined by its statistical positioning and normalized multivariate distance to a performance frontier. Both issues are represented in Fig. 1 for the simple case of six regions ($R_1, R_2, \ldots, R_6$) and two generic exposure indicators (y_1 and y_2). The line connecting the observed indicators' values for regions R_1, R_2, R_3 and R_4 (that has been notionally extended to the axes by the lines "$R_1y'_2$" and "$R_4y'_1$" to enclose the entire dataset) constitutes the performance frontier (i.e. maximum exposure among the regions represented in the sample dataset) and the benchmark for regions R_5 and R_6, which lie below that frontier. The regions supporting the frontier are classified as the most exposed according to their values in one or both indicators. The most exposed regions will have a performance score of 1, while regions R_5 and R_6, which are within this envelope, are less exposed than the others and score values between 0 and 1.

The non-compensatory exposure values for regions R_5 and R_6 are computed as follows (OECD/JRC, 2008):

$$de_i = \overline{0R_i}/\overline{0R'_i}, \tag{4}$$

where $\overline{0R_i}$ is the multivariate distance between the origin and the actual observed indicators' values for region i, and $\overline{0R'_i}$ is the distance between the origin and the projected regional values in the frontier of maximum exposure.

2.3. Analysis of drought vulnerability

Vulnerability depends critically on the context of the analysis, and the factors that make a system vulnerable to a natural hazard will depend on the nature of the system and the type of hazard in question (Cutter et al., 2003). However, there are factors that are likely to influence vulnerability to any hazard in different geographical and socio-political contexts (Peduzzi et al., 2009). These are developmental factors that include generic indicators such as poverty, health status, economic inequality and elements of governance (Brooks et al., 2005; UNDP, 2013). The focus on generic indicators is most important because they are valid for all type of exposed elements and thus do not alter with changes in the physical entities at risk.

In this paper, we adopt the framework proposed by UNISDR (2004) to drought vulnerability: a reflection of the state of the individual and collective social, economic and infrastructural factors of a region at hand. While these factors are mainly based on generic indicators that do not represent a complete description of vulnerability in relation to a specific exposed element, such factors may be viewed as the foundation on which regional plans for

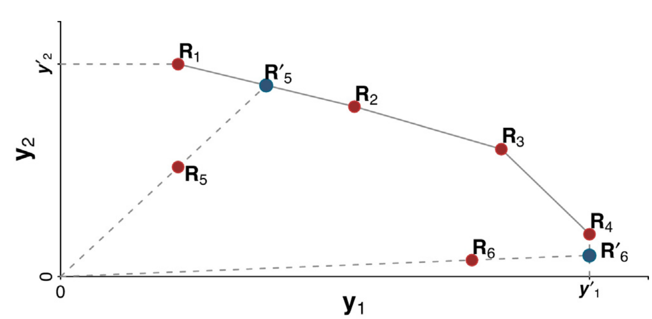

Fig. 1. Computation of a performance frontier in a simulated Data Envelopment Analysis (DEA) for six regions and two indicators. Red: observed indicator's values; Blue: projected indicators' values in the frontier of maximum exposure. (For interpretation of the references to color in this figure legend, the reader is referred to the web version of this article.)

reducing vulnerability and facilitate adaptation are built (Brooks et al., 2005; Naumann et al., 2014). Moreover, although the relative importance of different factors exhibit some geographic variation, they can be used independently as guidelines to stakeholders, policymakers and practitioners alike (Wilhite et al., 2014). Social vulnerability is linked to the level of well-being of individuals, communities and society; economic vulnerability is highly dependent upon the economic status of individuals, communities and nations; infrastructural vulnerability comprises the basic infrastructures needed to support the production of goods and sustainability of livelihoods (Scoones, 1998).

Vulnerability to drought is computed as a 2-step composite model that derives from the aggregation of proxy indicators representing the economic, social and infrastructural factors of vulnerability at each geographic location, as similar as for the Drought Vulnerability Index (DVI) (Naumann et al., 2014). In the first step, indicators for each factor are combined using a DEA model, as similar as for drought exposure (Section 2.2). In the second step, individual factors resulting from independent DEA analyses are arithmetically aggregated into a composite model of drought vulnerability (dv), as follows:

$$dv_i = \frac{Soc_i + Econ_i + Infr_i}{3}, \tag{5}$$

where Soc_i, $Econ_i$, and $Infr_i$ are the social, economic and infrastructural vulnerability factors for region i.

The proposed approach for deriving regional drought vulnerability follows the concept that individuals and populations require a range of "(semi-) independent" factors (characterized by a set of proxy indicators) to achieve positive resilience to impacts and that no single factor on its own is sufficient to yield all the many and varied livelihood outcomes that societies need to ensure subsistence. The selection of proxy indicators characterizing factors of drought vulnerability follows the criteria defined by Naumann et al. (2014): the indicator has to represent a quantitative or qualitative aspect of vulnerability factors to drought (generic or specific to some exposed element), and public data need to be freely available at the global scale. The emphasis in public data ensures that the final result can be validated, reproduced, and improved with new data by stakeholders. Moreover, as the results of an analysis performed by Naumann et al. (2014) have shown that removing or adding indicators within factors does not substantially change the relative vulnerability of regions to drought, we have decided to use the same set of indicators they have proposed for Africa (Section 3.1.3).

3. Data and methods

To map the global distribution of drought risk and compute the input regional scores of hazard, exposure and vulnerability, as well as to validate the applicability and robustness of the models proposed in Section 2, we have collected and pre-processed numerous datasets at different spatial resolutions. In this section, we describe the proxy data used for deriving the outputs of each model, the generalization of input data to a common minimum mapping unit (MMU), and the selection of countries and sub-national regions for overall drought risk analysis. In the sequence, we describe the methodology used for normalizing proxy indicators characterizing exposure and vulnerability to the range between 0 and 1, as well as the performance assessment to evaluate the robustness of the underlying models and the comparison criteria to validate their outputs against some standard composite approaches.

3.1. Data

3.1.1. Proxy for hazard

The computation of drought hazard is performed with monthly precipitation totals from the Full Data Reanalysis Monthly Product Version 6.0 of the Global Precipitation Climatology Centre (GPCC) (Becker et al., 2013). The GPCC was established in 1989 on request of World Meteorological Organization (WMO) and provides a global gridded dataset of monthly precipitation over land from operational in situ rain gauges based on the Global Telecommunications System (GTS) and historic precipitation data measured at global stations. The data supplies from 190 worldwide national weather services to the GPCC are regarded as primary data source, comprising observed monthly totals from 10,700 to more than 47,000 stations since 1901. The monthly datasets are spatially interpolated with a spherical adaptation of the robust Shepards empirical weighting method at 0.5° latitude/longitude grid spacing, from January 1901 to December 2010 (Becker et al., 2013).

3.1.2. Proxies for exposure

The nonparametric and non-compensatory DEA model of drought exposure is computed and validated on the basis of four spatially explicit geographic layers that completely cover the global land surface. These data are the following:

Global agricultural lands in the year 2000. This data collection represents the proportion of land area used as cropland in the year 2000. Satellite data from MODIS and SPOT-VEGETATION were combined with agricultural inventory data to create this product. The maps showing the extent and intensity of agricultural land use on Earth were compiled by Ramankutty et al. (2008) on a 5 min × 5 min latitude-longitude grid cell size (≈10 km × 10 km at the equator).

Gridded population of the world, version 4 (GPWv4). This data collection is a minimally-modeled gridded population dataset that is constructed by extrapolating the raw census counts from national or subnational input areal units of varying resolutions to estimates for the 2010 target year. The development of GPWv4 builds upon previous versions of the dataset (Tobler et al., 1997; Deichmann et al., 2001; Balk et al., 2006) and the current grid cell size of the product is 30 arc-seconds, or ≈1 km at the equator. There are other population data collections available in the literature and an alternative to this work could be LandScan (Dobson et al., 2000). The resulting LandScan distribution represents an ambient population, which integrates diurnal movements and collective travel habits into a single measure. Although this is desirable for purposes of emergency response to sudden hazards' impacts, such as earthquakes or floods, it is of limited added value for extremely low onset hazards, such as droughts that take between months to years to be established.

Gridded livestock of the world (GLW), v2.0. This data collection provides modelled livestock densities of the world, adjusted to match official national estimates for the reference year of 2005, at a spatial resolution of 3 min of arc (≈5 × 5 km at the equator). The freely accessible maps are created through the spatial disaggregation of sub-national statistical data based on empirical relationships with environmental variables in similar agro-ecological zones (Robinson et al., 2014).

Baseline water stress (BWS). This data collection is an indicator of relative water demand and is calculated as the ratio of local water withdrawal over available water supply for the baseline year of 2010 (Gassert et al., 2014a,b). Use and supply are estimated at the hydrological catchment scale, which polygons were extracted from the Global Drainage Basin Database (GDBD) (Masutomi et al., 2009).

3.1.3. Proxies for vulnerability

Vulnerability to drought is quantified by means of social, economic and infrastructural factors, which indicators are generic proxies that reflect the level of quality of different constituents of a civil society. Each factor is characterized by a set of proxy indicators that are generalized at the national and sub-national scales. Fifteen indicators, selected in accordance with the work of Naumann et al. (2014) and substantiated by the vulnerability studies of Scoones (1998), Brooks et al. (2005) and Alkire and Santos (2014), to cite but a few, are distributed among the three factors according to Table 1. Apart from "($Infr_1$) Agricultural irrigated land (% of total agriculture)", which is only valid for agricultural regions, all the other indicators are generic and valid for any region, independently of being exposed to one or more types of elements. Generic indicators of vulnerability factors are useful if we wish to undertake an analysis of risk that is based on different proxy indicators of exposure.

3.2. Defining the minimum mapping unit (MMU) of analysis

Sub-national administrative regions were selected to summarize the spatial distribution of proxy indicators representing vulnerability and exposure at the global level. To achieve our goal, we focused on the First Level of the 2015 Release of the Global Administrative Unit Layers (GAUL), an initiative implemented by Food and Agriculture Organization of the United Nations (FAO) within the Bill & Melinda Gates Foundation, Agricultural Market Information System (AMIS) and AfricaFertilizer.org projects (FAO, 2015). The GAUL compiles and disseminates the best available information on administrative units for all the countries in the world and maintains global layers with a unified coding system at country, first (e.g. departments) and second administrative levels (e.g. districts).

To summarize grid cell values of proxy indicators characterizing exposure at each sub-national administrative region, GPWv4 was converted to population density, GLW was converted to livestock density, BWS was averaged by weighted catchment area, and the proportion of rainfed crops was averaged by the number of grid cells at each region. Concerning the geographic layers of proxy indicators characterizing infrastructural vulnerability, $Infr_1$ was averaged by weighted catchment area and $Infr_3$ was converted to road density for each sub-national administrative region, while $Infr_1$ was computed as the proportion of total agricultural land for agricultural regions. Finally, sub-national administrative regions inherited the values of proxy indicators characterizing socioeconomic vulnerability factors for the nations in which are included.

3.3. Masking sub-national administrative regions

The proxy indicators of exposure and vulnerability that have been used as input for the respective models were compiled for 170 countries and 2515 sub-national administrative regions – approximately 67% of the total emerged lands (Fig. 2). We decided to remove sub-national administrative regions from the analysis if: are not covered by geographic layers of exposure and/or infrastructural vulnerability; are not described by social and/or economical indicators of drought vulnerability; are entirely covered by surface water bodies. Moreover, on account of the fact that dealing with drought concepts in arid and cold areas is physically meaningless (Lyon and Barnston, 2005; Carrão et al., 2014; Spinoni et al., 2015), we used the global aridity index dataset from Spinoni et al. (2015) to exclude also the sub-national administrative regions that are included in these areas from drought risk analysis.

Although several guidelines on data treatment for missing values could have been used for predicting the scores of some raw indicators for the regions not covered by geographic layers of vulnerability or exposure, such as filling by explicit modeling using an unconditional median imputation of each indicator in the entire dataset (e.g. Naumann et al., 2014; OECD/JRC, 2008), we rather chose to remove these regions from the analysis. We consider that missing data are questionable in quantitative social research and imputation methods can lead to incorrect inferences that bias the outcomes for regions with incomplete scores. In fact, we see that a simple statistical imputation of socioeconomic indicators' values

Table 1
Indicators of drought vulnerability in detail: corresponding factors, data sources, reference dates and correlation to the overall vulnerability.

Factors	Indicator	Scale	Correlation	Year	Source[a]
Economic	($Econ_1$) Energy Consumption per Capita (Million Btu per Person)	Country	Negative	2014	U.S. EIA
	($Econ_2$) Agriculture (% of GDP)	Country	Positive	2000–2014	World Bank
	($Econ_3$) GDP per capita (current US$)	Country	Negative	2000–2014	World Bank
	($Econ_4$) Poverty headcount ratio at $1.25 a day (PPP) (% of total population)	Country	Positive	2000–2014	World Bank
Social	(Soc_1) Rural population (% of total population)	Country	Positive	2000–2014	World Bank
	(Soc_2) Literacy rate (% of people ages 15 and above)	Country	Negative	2000–2014	World Bank
	(Soc_3) Improved water source (% of rural population with access)	Country	Negative	2000–2014	World Bank
	(Soc_4) Life expectancy at birth (years)	Country	Negative	2000–2014	World Bank
	(Soc_5) Population ages 15–64 (% of total population)	Country	Negative	2000–2014	World Bank
	(Soc_6) Refugee population by country or territory of asylum (% of total population)	Country	Positive	2000–2014	World Bank
	(Soc_7) Government Effectiveness	Country	Negative	2013	WGI
	(Soc_8) Disaster Prevention &Preparedness (US$/Year/capita)	Country	Negative	2014	OECD
Infrastructural	($Infr_1$) Agricultural irrigated land (% of total agricultural land)	5 arc minute raster	Negative	2008	FAO
	($Infr_2$) % of retained renewable water	Hydrological catchment	Negative	2010	Aqueduct
	($Infr_3$) Road density (km of road per 100 sq. km of land area)	Vector	Negative	2010	gROADSv1

[a] Data sources:
World Bank, http://data.worldbank.org/products/wdi.
U.S. Energy Information Administration (EIA), http://www.eia.gov/.
Worldwide Governance Indicators (WGI), http://info.worldbank.org/governance/wgi/index.aspx#home.
Organisation for Economic Co-operation and Development (OECD), http://stats.oecd.org/.
Food and Agriculture Organization (FAO), http://www.fao.org/nr/water/aquastat/main/index.stm.
Aqueduct, http://www.wri.org/our-work/project/aqueduct.
Global Roads Open Access Dataset (gROADSv1), http://sedac.ciesin.columbia.edu/data/set/groads-global-roads-open-access-v1.

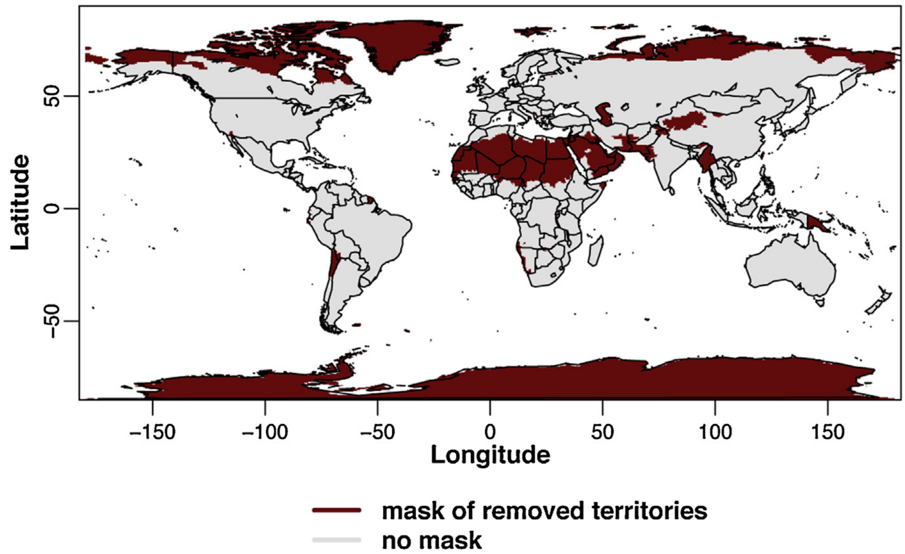

Fig. 2. Territories excluded from global drought risk analysis.

will not provide a representative real state of individual and collective social, economic and infrastructural dimensions for missing regions. Missing values could be better assigned through expert knowledge, which has not been part of this study.

3.4. Normalization of exposure and vulnerability indicators

After summarizing raw values of indicators of drought exposure and drought vulnerability for all sub-national administrative regions not removed by the processes defined in Section 3.3, we normalized indicators among the remaining regions for display and aggregation. The normalization has been made by taking into account the maximum and minimum value of each indicator across all regions in order to guarantee that input model values have an identical range between 0 and 1 (OECD/JRC, 2008). Regarding indicators of exposure and those with a positive correlation to the overall vulnerability (see Table 1), the normalized input values are calculated according to the general linear transformation (Naumann et al., 2014):

$$Z_i = \frac{X_i - X_{\min}}{X_{\max} - X_{\min}}, \tag{6}$$

where X_i represents the indicator value for sub-national region i, $X_{\min}$ and $X_{\max}$ the respective minimum and maximum values across all regions. In some cases there is an inverse relationship between vulnerability and indicators (e.g. GDP per capita, adult literacy rate, or road density). For indicators with negative correlation to the overall vulnerability (see Table 1), a transformation was applied to link the lowest indicator values with the highest values of vulnerability, as follows (Naumann et al., 2014):

$$Z_i = 1 - \frac{X_i - X_{\min}}{X_{\max} - X_{\min}}, \tag{7}$$

3.5. Performance evaluation of exposure and vulnerability models

In order to assess the robustness of the predictive models of drought exposure and vulnerability, we compared their outputs to the outputs of alternative models built with weighting and aggregation schemes inspired by composite measures already existing in the literature, namely the Human Development Index (HDI) (UNDP, 2013), the Drought Vulnerability Index (DVI) (Naumann et al., 2014) and the Multidimensional Poverty Index (MPI) (Alkire and Santos, 2014). As similar as for the outputs of exposure and vulnerability models, the outputs of these composite measures are not directly observed but rather inferred (through different mathematical models) from proxy indicators: the HDI is the geometric mean, the DVI is the arithmetic mean and the MPI is the product of proxy data characterizing indicators of socioeconomic conditions. Although the theoretical advantages/ disadvantages of these composite measures are described in the literature, we decided to perform a statistically sound comparison of models based on different weighting and aggregation schemes to evaluate their empirical performance for computing drought exposure and vulnerability. We did not perform an empirical evaluation of the WASP-Index for drought severity computation as its good performance for monitoring standardized monthly precipitation deficits has already been reported by Lyon and Barnston (2005) and Andrade and Belo-Pereira (2015), to cite but a few.

For the case of regional drought exposure, it is desirable that the final composite measure does not trade-off high values in some indicator(s) by low values in some other indicator(s) (as described in Section 3.1.2). We aim at selecting a multidimensional measure of exposure that preserves the magnitude of individual indicators and simultaneously increases with an increment of the exposed elements. In other words, we consider that a region is highly exposed if there is a high amount of one, few or many types of exposed assets. Therefore, to test the robustness of the proposed non-compensatory DEA model of drought exposure ($DEAde_i$), we compare it to compensatory models that interpret regional exposure as the arithmetic average ($AAde_i$), the geometric average ($GAde_i$) and the product (Pde_i) of normalized input indicators. The comparison is performed by means of a correlation analysis between the maximum of the normalized indicators per sub-national administrative region ($max\{Z_{k,i}\}$) and the regional outputs of the four concurrent measures of exposure. We compare the models to the maximum of the normalized indicators to evaluate which preserves better the magnitude of individual indicators. The model achieving higher correlation with $max\{Z_{k,i}\}$ is able to more accurately identify the regions of high exposure, independently of being exposed to one, few or many types of droughts.

The problem of evaluating the aggregation and weighting schema that performs better for modeling drought vulnerability can be statistically compared to a machine learning task of inferring the best function to describe a hidden structure (i.e.

cluster) from unclassified data. For the case of drought vulnerability, the order and stability of regional rankings, $Rank(dv_i)$, are *a priori* unknown and the question of identifying an appropriate composite measure for their classification is ill-posed, in that the output rankings are not directly observed but are rather inferred and may have more than one satisfactory solution (Lange et al. 2004). Therefore, we used an internal variance minimization technique of unsupervised cluster stability, i.e. the minimum distance to cluster centroid or median ranking (Levine and Domany, 2001), to evaluate the performance of compared composite measures of drought vulnerability. The distance criteria $\overline{Rank}(d_v)$ is computed as:

$$\overline{Rank}(d_v) = \frac{1}{N}\sum_{i=1}^{N}\left|Rank_{\tilde{i}} - Rank_i(dv)\right|, \tag{8}$$

where $Rank_{\tilde{i}}$ is the median rank of the ensemble computed for region i with the investigated model configurations, and $Rank_i(dv)$ is the rank estimated by model dv for the same region i. This classification method of cluster stability places vulnerabilityrankings that are computed with different composite measures for each region i in individual (single) clusters, and uses the minimum average distance to the regional median rankings (or cluster centroids) to determine the composite measure of drought vulnerability that gives more stable regional outputs (Lange et al., 2004). This statistical method based on the median ranking is named “consensus ranking” in social choice theory, as well as in discrete mathematics (Arrow, 1951). It is commonly used as a majority rule voting system based on the median to select a consensus ranking when multiple respondents supply preferences concerning a set of alternatives (Cook, 2006; Heiser and D'Ambrosio, 2013). In this study, we compare the model of drought vulnerability proposed in Eq. (5) to seven alternative models that are based on (A) arithmetic, (G) geometric, or (P) product composite of factors derived from (W) weighted (i.e. proportional weights) or (NW) non-weighted (i.e. equal weights) aggregation of proxy indicators by means of (C) compensatory (i.e. arithmetic average) and (NC) non-compensatory (i.e. DEA) methods.

4. Results and discussion

In this section, we present the global maps of drought risk and its determinants of hazard, exposure and vulnerability, as well as the results of the evaluation performed to assess the robustness of the proposed models. Since the approach for computing drought risk is relative and each region is part of a global community that interact, share and support each other social and economically, then we decided to conduct the analysis of the results from a global to a continental perspective, and finally to look at the national and sub-national scales of risk and its determinants in South-Central America.

Given the significant reliance of South-Central American economies on rainfed agricultural yields (rainfed crops contribute more than 80% of the total crop production in South-Central America (FAO, 2014)), and the exposure of agriculture to a variable climate, there is a large concern in the region about present and future climate and climate-related impacts (Trenberth and Stepaniak, 2011). South-Central American countries have an important percentage of their GDP in agriculture (10% average FAO, 2014), and the region is a net exporter of food globally, accounting for 11% of the global value (Yadav et al., 2011). According to the agricultural statistics supplied by the United Nations Food and Agriculture Organization (FAO, 2014), 65% of the world production of corn and more than 90% of the world production of soybeans are grown in Argentina, Brazil, the United States and China. The productivity of these crops is expected to decrease in the extensive plains located in middle and subtropical latitudes of South-America (e.g. Brazil and Argentina), leading to a reduction in the worldwide productivity of cattle farming and having adverse consequences to global food security (Magrin et al., 2007; Llano et al., 2012).

4.1. Drought hazard

Fig. 3 shows the world map of drought hazard computed for the events taking place in the period between January 1901 and December 2010. Overall, it is noticeable a match between the geographic distribution of global drought hazard, as computed with the WASP index, and the wide range of global dry regions, as

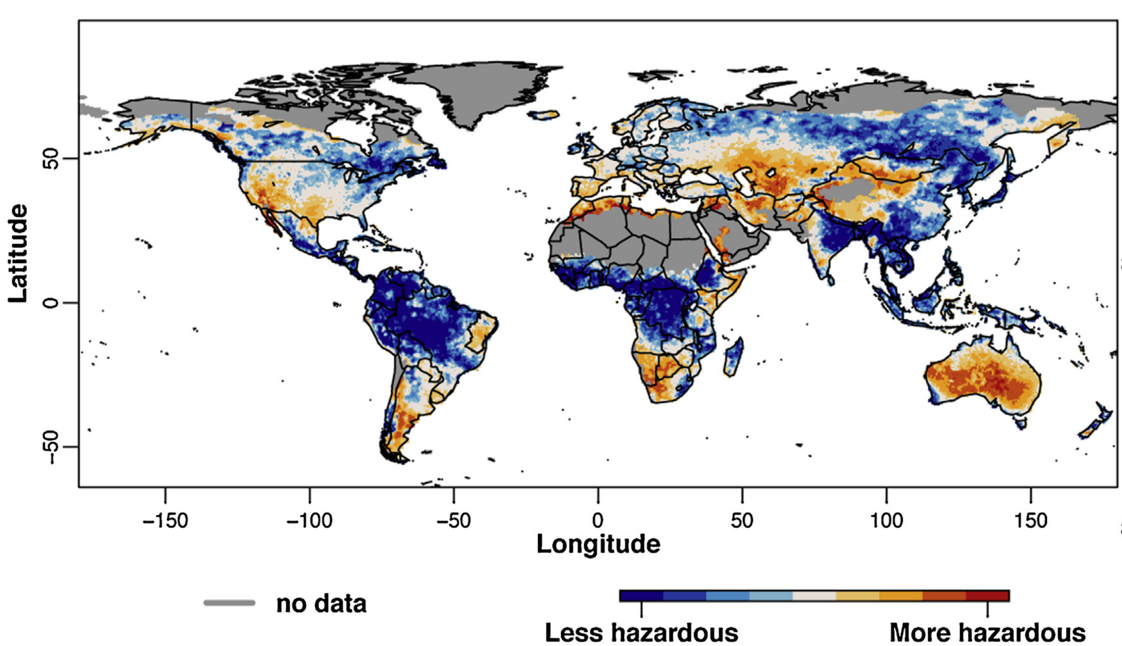

Fig. 3. Global map of drought hazard.

depicted by the global map of aridity computed by Spinoni et al. (2015). Our experiments are consistent with previous results presented by Seager et al. (2007), Dai (2011), Spinoni et al. (2014), and Güneralp et al. (2015): drought hazard is generally high for semiarid areas, such as Northeastern and Southern South America, Northern, Southwestern and Horn of Africa, Central Asia, Australia, West U.S. and the Iberian Peninsula; and low for tropical regions, such as the Amazon, Central Africa and Southern Asia.

Perhaps more interestingly though is the fact that some humid areas in wealthy regions, such as Northwest France, Southeast England, Southeast Brazil, Uruguay, and Southeast U.S., which are extensively exploited for agriculture and livestock farming, show some moderate to severe drought hazard. Since future climate trends suggest an increase of drought frequency and intensity for those regions (Russo et al., 2013), then there is an aggravated risk for food security in the future and a need to establish or reinforcing preparedness plans for drought monitoring, mitigation and adaptation in those regions.

Looking at the regional scale and the results presented for South-Central America, the semi-arid regions of Northeast Brazil, Southern Argentina, the Gran Chaco (Northern Argentina, South-eastern Bolivia and North-Western Paraguay), and North-Eastern and -Western Mexico are immediately identified as hot spots subject to severe drought conditions. On the other hand, the tropical areas of North-West Amazon rainforest, the fully humid subtropical zone of Southeast Brazil and the temperate oceanic area of Southern Chile are less prone to severe drought conditions.

Let us now look in detail at the link between drought hazard mapped with the WASP index and the drought hazard pattern at the sub-national scale. In 1936, the Semi-Arid Region of Northeast Brazil (SARNB, black polygon in Fig. 3) was officially recognized by the federal government as having a common recurrence of drought episodes and it was delimited under the name of Drought Polygon to augment the governmental support to the resident populations living there (Brasil-MMA, 2004; Brasil-MI/MMA/MCT, 2005). The results shown in Fig. 3 confirm that the geographic distribution of drought hazard computed with the WASP for Northeast Brazil is overall consistent with the geometric shape of the official Drought Polygon (Brasil-MI/MMA/MCT, 2005). The probability of exceeding the median severity of historical global drought events is at least double inside the Drought Polygon than in its vicinity (between 20 and 75% inside and $\leq$10% outside). These results seem to emphasize the validity of the hazard model and lend additional support to its use for estimating drought hazard from national to global scales.

4.2. Drought exposure

In Fig. 4, we present the map of global drought exposure computed at the sub-national level with the non-compensatory DEA model. Our results anticipate that inhospitable regions like deserts, tundras, and tropical forests are the least exposed to drought worldwide. In fact, there is an antagonism between the global distribution of major human settlements, livestock farming and agricultural activities, and those regions, thus sustaining the overall accuracy of the proposed non-parametric model. Over the globe, drought exposure is higher for Eastern U.S., Southern Europe, India, East China and Nigeria.

Let us look in more detail at the spatial distribution and intensity of exposure to drought in South-Central America. As similar as for the global context, the arid and semiarid regions of South-Western Argentina, North and Southern Chile, and North-Western Mexico, as well as the fully humid Amazonian regions are less exposed to drought. On the other hand, the most exposed sub-national regions are located in South to Southeast Brazil, North-West Argentina, Cuba, Southeast Mexico and some scattered areas in the west coast of South-America. According to Parré and Guilhoto (2001), South and Southeast Brazil produce together more than 70% of the crops in the country: South Brazil is the largest tobacco producer and the world's largest exporter, whereas Southeast produces almost 50% of the nation's fruit and hosts 60% of agribusiness companies. In Argentina, the most exposed areas are the Chaco plain – fertile lowland in the Northern region with subtropical rainforests and cotton farms; and the central Pampas – flat, fertile plains (a mix of humid and semi-arid areas) which provide much of Argentina's agriculture including raising of sheep and cattle, as well as wheat, corn, soybean and fodder crops (Llano et al., 2012). In the case of the tropical rain forest of Southeast Mexico, 50% of its area has been cut down and extensive natural pastures and field crops have been established in its place over the

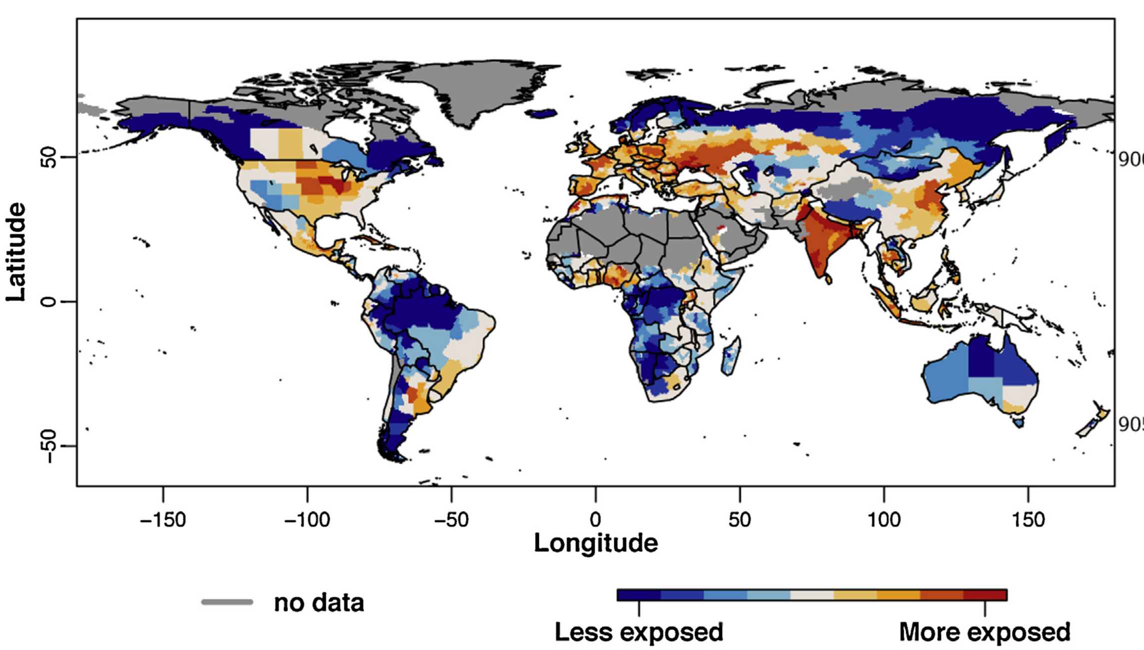

Fig. 4. Global map of drought exposure.

last 40 years (Alvarez-Buylla Roces et al., 1989). Under these particular conditions and together with population increases of up to 207.1% for some municipalities (Alvarez-Buylla Roces et al., 1989), multispecies agroforestry cropping systems with cattle raising have developed and are a means by which the peasant families are able to maintain self-subsistence production.

Interesting also to note that exposure to drought in Cuba is higher than for other South-Central American countries. While 60% of its land is appropriate for agriculture, the average agricultural area for the region is just about 34% (FAO, 2014). Moreover, the geographical region of the Central American Dry Corridor (CADC), which extends over Guatemala, El Salvador, Honduras and Nicaragua, is more exposed to drought than the sub-national regions of the remaining Central American countries not included in the CADC. Even that Central America is located in a tropical region with low hydric stress, drought risk is mentioned in many studies related to the CADC, as the impacts of droughts usually threaten food security in the region. It is common to observe widespread impacts to these extreme events due to high exposure related to subsistence agriculture and livestock (Rodríguez et al., 2012; van der Zee Arias et al., 2012a,b). Indeed, from a total of 10.5 millions of people that live in the rural areas of the dry tropics (almost all in Nicaragua, Honduras, and Guatemala), close to 60% depend on subsistence agriculture and have deteriorated livelihoods (van der Zee Arias et al., 2012a).

Performance evaluation. To statistically evaluate the presented results, we compared the proposed non-compensatory DEA model of drought exposure to compensatory models that interpret regional exposure as the arithmetic average ($AAde_i$), the geometric average ($GAde_i$) and the product (Pde_i) of normalized proxy indicators. A correlation analysis was performed with the maximum of the normalized exposure indicators per sub-national region and the outputs of the exposure models to analyze how individual indicators were contributing to the distribution of overall exposure values. The results presented in Fig. 5 show a good agreement between the maximum value of normalized indicators per sub-national region and the outputs of $AAde_i$, $GAde_i$ and $DEAde_i$, with correlation coefficients above 0.9 at the 5% significance level. On the other hand, we immediately perceive that the product (Pde_i) is not adequate for computing exposure from a multidimensional set of proxy indicators: its correlation value with the maximum of normalized exposure indicators is around zero, and it does neither preserve the magnitude of individual indicators nor increase with an increment of exposed elements.

Since correlation values are positive for $AAde_i$, $GAde_i$ and $DEAde_i$, it shows that as long as the values of at least one exposure indicator

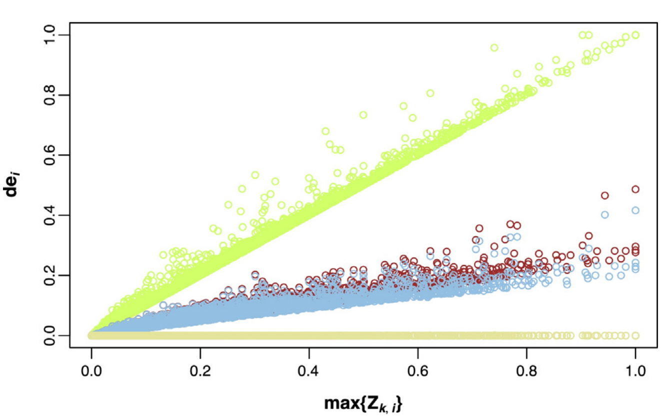

Fig. 5. Exposure values as function of the maximum indicators' values per sub-national region: arithmetic average ($AAde_i$, red); geometric average ($GAde_i$, blue); product (Pde_i, beige); DEA ($DEAde_i$, green). (For interpretation of the references to color in this figure legend, the reader is referred to the web version of this article.)

increases, exposure will increase as well from all models. Nevertheless, and although the three models show a very high positive correlation with the maximum value of the four normalized indicators, the results from Fig. 5 highlight the fact that the compensatory approaches minimize the variability of exposure values to the interval [0, 0.5]. The reason is that low values in one or more indicators will reduce regional exposure, even if the values for the remaining indicators are high. Therefore, these models do not preserve the magnitude of individual indicators and are not adequate for computing drought exposure.

To analyze the discourse of the previous paragraph, let us look at Table 2. The rows are representative of the 11 sub-national regions with the highest $AAde_i$ values, and are ranked by their descending order (column "C"). The analysis of the values in Table 2 shows that the compensatory model suffers from a number of pitfalls: as it assumes that low values in one or more indicators counterbalance the high values on the other indicators, it lessens regional exposure and smooths regional variability from input indicators. Therefore, the compensatory approach does neither guarantee the representation of regional extreme exposure values, nor the absolute contribution of single indicators to regional exposure. Let us look in detail, for example, at Dki Jakarta region, Indonesia. Although this is the worldwide region with the highest population density (as mapped by the GPWv4 dataset, Section 3.1.2), its compensatory exposure value is almost half of that for Rangpur region, Bangladesh, which is characterized by lower population density. The compensatory approach considers that Dki Jakarta is less exposed because only one indicator is showing high values, i.e. population density, whereas Rangpur region has also an high percentage of area covered by agriculture. On the other hand, since the non-compensatory approach looks at single indicators independently, it classifies Dki Jakarta as exposed as Rangpur.

4.3. Drought vulnerability

In Fig. 6, we present the global drought vulnerability map derived from an arithmetic composite model combining (a) social, (b) economic and (c) infrastructural factors computed with a non-compensatory aggregation schema of vulnerability indicators. Overall, results indicate that Central America, Northwest of South America, Central and South Asia, and almost all Africa – with the exception of South Africa, are the most vulnerable regions to drought worldwide. Indeed, our results match the outcomes of Brooks et al. (2005), which classified nearly all nations situated in sub-Saharan Africa among the most vulnerable to climate hazards in the world. On the other hand, the wealthiest regions in the world are amongst the less vulnerable to drought, namely Western Europe, North America and Oceania.

A detailed analysis of the factor maps presented in Fig. 7, suggests that relatively high values of vulnerability to drought in Africa and Central America are function of simultaneously low infrastructural, social and economic capacity. On the other hand, for South America and Central Asia, vulnerability is mainly due to a lack of infrastructural capacity, whereas in South Asia there is insufficient socioeconomic capacity to manage the impacts of drought events.

Regarding South-Central America, one of the most striking results is the high vulnerability spot located at the middle latitude, namely covering the countries of Guatemala, El Salvador, Honduras and Nicaragua. Central America's population is growing rapidly, with average annual growth rates over the past ten years ranging from 1.6% in Panama to 2.6% in Honduras and Nicaragua (Pielke et al., 2003). Population growth increases exposure, as there are more people for a disaster to impact (as depicted in Section 4.2), but it is also related to poverty and this is a critical indicator

Table 2
Sub-national regions with highest drought exposure derived from a compensatory aggregation scheme of indicators and respective: exposure derived from a non-compensatory aggregation scheme and normalized indicators' values.

Region	Country	NC[a]	C[b]	Pop[c]	Crop[d]	Livestock[e]	IndDom[f]
Rangpur	Bangladesh	1.000	0.487	0.074	1.000	0.870	0.002
Rajshahi	Bangladesh	0.965	0.466	0.079	0.944	0.840	0.002
Khulna	Bangladesh	0.775	0.371	0.063	0.770	0.649	0.001
Dhaka	Bangladesh	0.871	0.366	0.118	0.562	0.782	0.001
Kano	Nigeria	0.764	0.357	0.041	0.713	0.672	0.003
Ha Noi City	Vietnam	1.000	0.332	0.312	0.098	0.914	0.005
Katsina	Nigeria	0.822	0.320	0.022	0.497	0.760	0.001
West Bengal	India	0.777	0.319	0.081	0.481	0.706	0.006
Haryana	India	1.000	0.300	0.042	0.075	0.903	0.181
Delhi	India	0.958	0.297	0.740	0.084	0.253	0.110
Dki Jakarta	Indonesia	1.000	0.297	1.000	0.021	0.142	0.024

[a] NC: Non-compensatory.
[b] C: Compensatory.
[c] Pop: Population density (people per sq. km of land area).
[d] Agr: Crop land (% of total land area).
[e] Livestock: Livestock density (domestic animals per sq. km of land area).
[f] IndDom: Industrial and domestic water withdrawal (% of total renewable water resources).

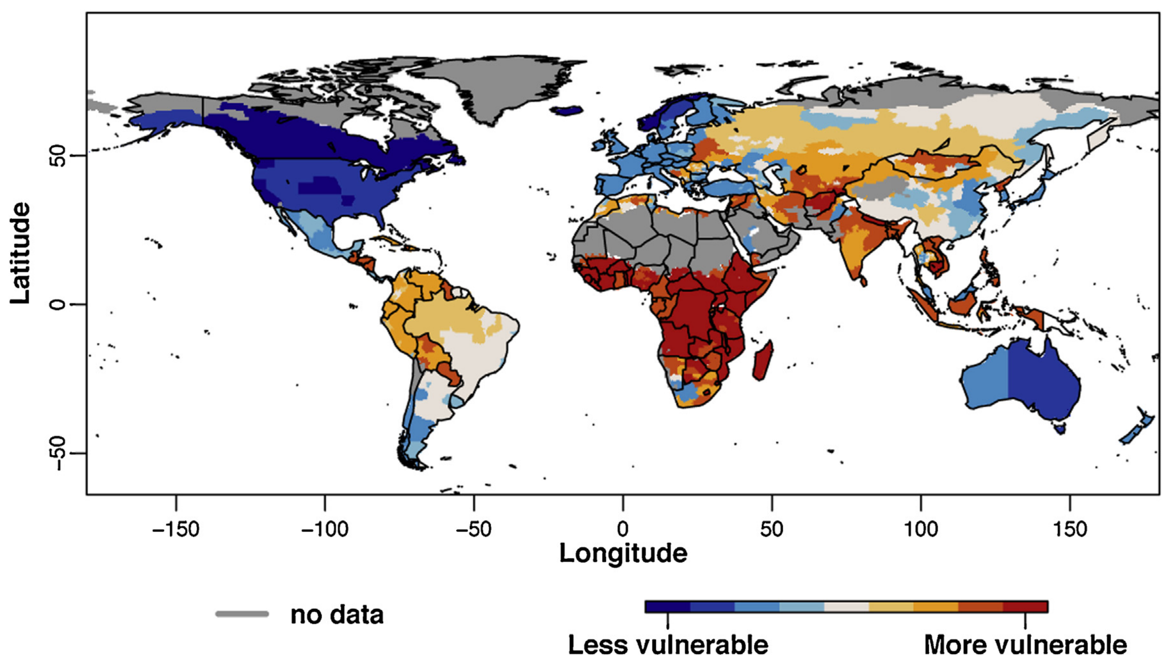

Fig. 6. Global map of drought vulnerability.

underlying the economic vulnerability factor (Lavell, 1994). In fact, an inverse relationship has been demonstrated between per capita GDP and total fertility rates, with these countries having some of the highest fertility rates among the poorest in the region (Pielke et al., 2003). Central American countries show also the highest percentage of rural population for the region. Rural societies may be more vulnerable to drought because of lower incomes and more dependence on a locally based resource economy, such as on self-subsistence agriculture (Cutter et al., 2003).

It is also interesting to highlight some intra-national differences of vulnerability to drought at sub-national administrative level, which are mainly due to spatial discrepancies of the infrastructural indicators within a country. For example, North-West Brazil is more vulnerable to drought than the Southeastern part of the country: this discrepancy is mainly due to limited road network, and reduced water storage and irrigation structures in the regions that are covered by the tropical Amazon forest.

Performance evaluation. To statistically evaluate the validity of the global results presented in Fig. 6, we compared the regional vulnerability ranks derived with the model proposed in Eq. (5) to alternative composite statistics and aggregation schema, as described in Section 3.5. The criterion to evaluate the robustness of the different models is internal and based on the distance between the respective regional rankings and the median regional ranking of the ensemble set defined by the outputs of all investigated models. In Table 3, we present the complete list of mean absolute distances of the eight concurrent models of vulnerability to the median rank. In Fig. 8, we present the range of vulnerability ranks computed for sub-national regions by means of all compared models (grey vertical lines); regions are sorted horizontally (from left to right) in ascending order of the median rank computed from the ensemble of all models.

Overall, regional rankings derived from the non-compensatory aggregation of indicators within vulnerability factors are closer to

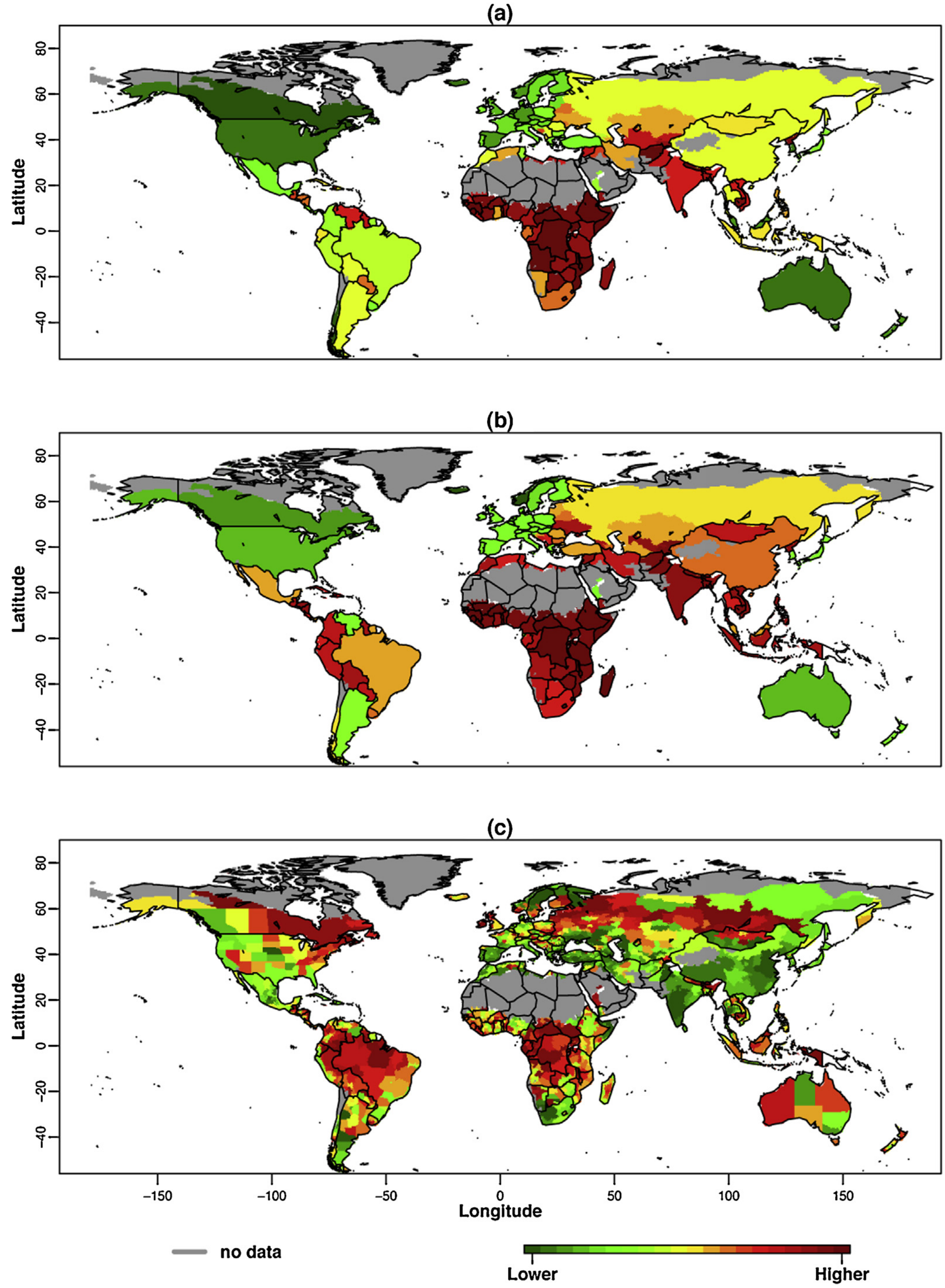

Fig. 7. Global maps of drought vulnerability factors computed with the DEA approach: (a) social; (b) economic; (c) infrastructural.

Table 3
Mean distance between the regional rankings of vulnerability models and the median regional ranking of the ensemble set. NW: Non-Weighted; W: Weighted; A: Arithmetic; G: Geometric; P: Product; NC: Non-Compensatory; C: Compensatory.

	NW-A-NC	NW-G-NC	NW-P-NC	NW-A-C	NW-G-C	NW-P-C	W-A-NC	W-A-C
R_{d_v}	81.67	83.88	96.59	181.23	146.59	96.15	119.57	93.12

the median of regional ranks. Indeed, the models showing shortest and largest distances are, respectively, the model proposed in Eq. (5) and the non-weighted arithmetic composite of vulnerability factors derived with a compensatory aggregation scheme of indicators. The output regional rankings derived from these models are presented, respectively, by green and red dots in Fig. 8. These outcomes suggest that the model proposed in Eq. (5) is more stable and robust than the concurrent models, and best representative of the unknown regional vulnerability rankings according to the median voting principle.

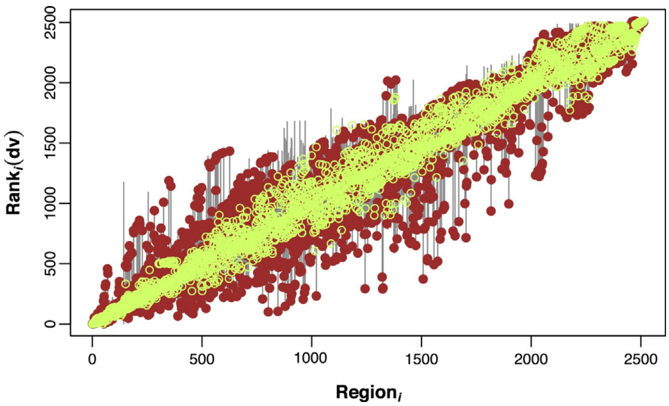

Fig. 8. Vulnerability to drought for sub-national regions ordered by the median ensemble rank: (black grey lines) range of ensemble rank values; (red dots) rank of sub-national regions based on the model with maximum distance to median rank; (green dots) rank of sub-national regions based on the model with minimum distance to median rank. (For interpretation of the references to color in this figure legend, the reader is referred to the web version of this article.)

4.4. Drought risk

In Fig. 9, we present the global map of drought risk computed as the product of the maps presented in Figs 3, 4, and 6, as previously defined in Eq. (1). As expected, one immediately perceives that the regions less affected by severe drought events, such as tundras, deserts, and tropical forests (Fig. 3), which correspond also to the regions with lower or no exposure to drought (Fig. 4), have null or lower drought risk. Since the remaining regions are subject to more severe drought events, then the risk increases as function of the total exposed entities and the coping capacity (i.e. the opposite reverse of vulnerability presented in Fig. 6) of individuals and society to absorb or recover from drought impacts. For example, although some regions in the U.S., Europe and Central-South Asia are similarly exposed and frequently affected by severe drought events, the drought risk is lower for the U.S. and Europe as they are less vulnerable to drought.

In Fig. 10, we present the frequency distribution of hazard, exposure and vulnerability for the regions categorized in the first, second, third and fourth quarters of drought risk computed over the globe. The analysis of the contribution of each determinant of drought risk for the spatial distribution of its magnitude is an important outcome to governments, international and regional organizations, and nongovernmental organizations, amongst others, for implementing a drought policy. It is a convenient instrument that provides a clear set of principles or operating guidelines to govern the management of drought and its impacts at multiple scales. Of course these results are open to further interpretation based on the available data and respective spatial resolutions. For example, it is interesting to note that the interquartile range and median of regional drought hazard distributions are similar for all categories of drought risk. This demonstrates that the regional values of drought risk do not increase with the intensification of drought frequency alone. Indeed, our results are indicating that regional exposure behaves as the key determinant of drought risk distribution – risk values converge asymptotically to their maximum as a function of the exponential increase of exposed elements at a region. On the other hand, it is also remarkable to observe that the lower quartiles of vulnerability are always above 0.3 for all drought risk categories, thus confirming that the assets within all regions are vulnerable to drought (Downing and Bakker, 2000). Nevertheless, the lower and upper quartiles of vulnerability distributions show a moderate increase at higher risk categories and the interquartile range decreases for the highest drought risk category. This demonstrates that drought risk also increases at the regions more vulnerable to drought. Therefore, since drought hazard can occur anywhere and physical entities are exposed to drought everywhere, then drought risk may be mitigated through reducing regional vulnerability values at the social, economic or infrastructural factors.

To better depict the contribution of vulnerability factors to drought risk, let us look at their frequency distributions for the regions categorized in the first, second, third and fourth quarters of drought risk computed over the globe (Fig. 11). First, it is interesting to note that most regions lack infrastructural capacity to cope with the impacts of drought hazards. As some of the proxy indicators of infrastructural vulnerability used in this study are only valid for agricultural areas, then our results indicate that a reduction in regional drought risk may be rapidly achieved through increasing irrigation and water harvesting systems for those regions. On the other hand, it is important to stress that the economic vulnerability factor seems to contribute more to global drought risk than the social factor – the first shows medium to high

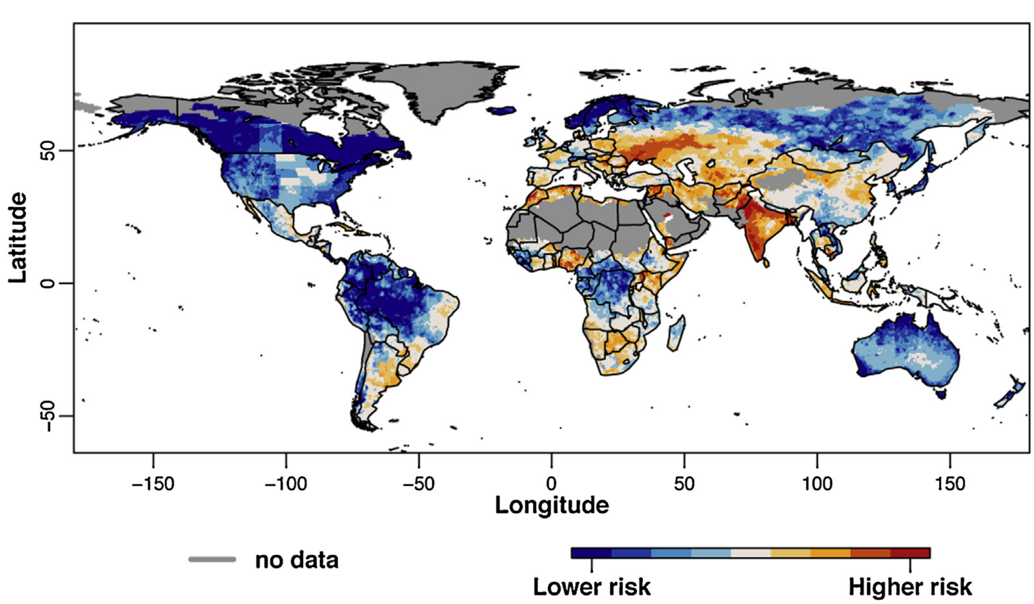

Fig. 9. Global map of drought risk.

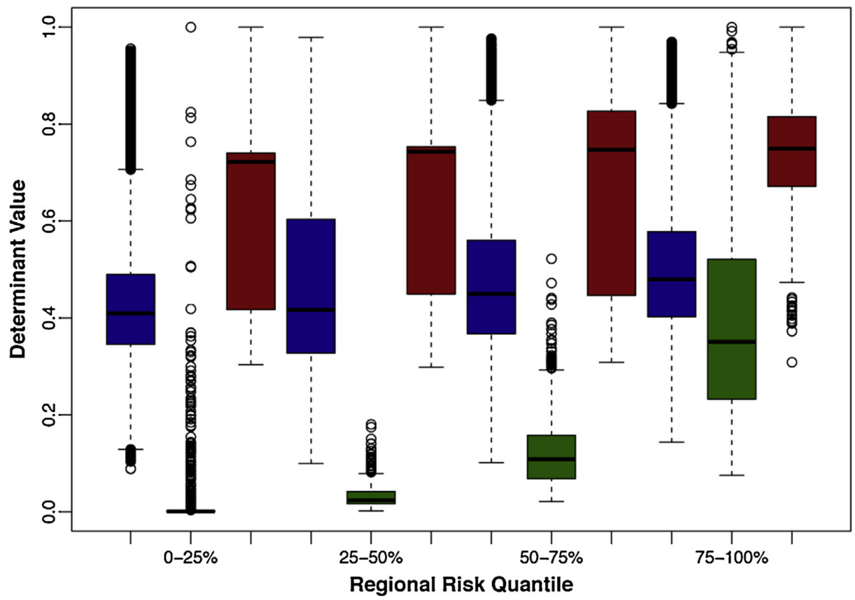

1135

Fig. 10. Frequency box-plot distributions of drought hazard (blue), exposure (green) and vulnerability (red) values for the regions in the 1st (0–25%), 2nd (25–50%), 3rd (50–75%) and 4th (75–100%) quarter of drought risk values computed over the globe. (For interpretation of the references to colour in this figure legend, the reader is referred to the web version of this article.)

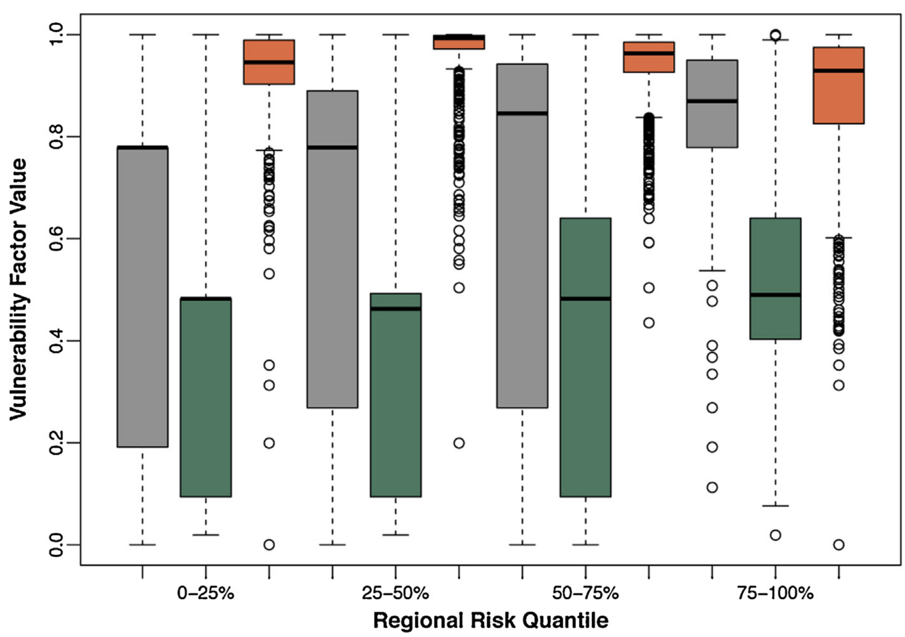

Fig. 11. Frequency box-plot distributions of economic (grey), social (marine) and infrastuctural (orange) values for the regions in the 1st (0–25%), 2nd (25–50%), 3rd (50–75%) and 4th (75–100%) quarter of drought risk values computed over the globe. 0 = less vulnerable; 1 = more vulnerable. (For interpretation of the references to color in this figure legend, the reader is referred to the web version of this article.)

values at all categories of drought risk, whereas the latter presents low to medium values. These results suggest that governance standards and literacy rates over most regions of the world are less associated to drought risk than their economic wealth and poverty headcount ratios. Therefore, reduction in drought risk may also be achieved by diversifying regional economies on different sectors of activity and reducing the added value of agriculture to their GDP.

To finish, let us regard again the problem of drought risk in South-Central America. We draw attention to two particular regions: the CADC and the Southeastern of South America (SESA), including Southeast Brazil, Northeast Argentina and Uruguay. The common determinant of risk is drought exposure: it is similar and higher than for neighboring nations because both regions are densely populated (rural communities in CADC and urban communities in SESA) and resemble by having large areas allocated for agricultural production (self-subsistence in CADC in contrast to cash crops in SESA). The distinctive determinants are the time pattern of hazard and vulnerability factors. Drought risk in SESA is higher because precipitation deficits usually spread over several months and years (Carrão et al., 2014). Since those regions are the pillars of primary sectors of activity of the respective countries, then the potential long-term failure of regional water resources systems eventually causes serious economic and social disruptions at the national scale. Indeed, the reduction of 20–23% of precipitation over Southeastern Brazil from 2012 to 2015 was enough to raise serious drought disasters at the country level (Getirana, 2016). On the other hand, drought risk in Central America scores high because the economic subsistence of typical rural communities depends on yearly crop yields. As rainfed agricultural production and water resources management in dry regions are especially sensitive to short midsummer droughts (also known as *canícula*), these mild intensity events that occur during crop growing season can have serious impacts on local populations that do not have the infrastructural and economic resources to cope with it (Hernández et al., 2008).

The results of this analysis highlight that although CADC and SESA are different in political guidance, socioeconomic structure and climate variability, both regions require great attention from governance to create more resilient societies, maintain the sustainability of their natural resources and ensure food security. On the one hand, disaster risk reduction for CADC may be achieved by governmental support to the establishment and/or improvement of local irrigation and water harvesting infrastructures, as well as through capacity-building activities directed at community training on sustainable agriculture and rural development under climate change conditions. On the other hand, progress on disaster risk reduction for SESA may benefit from improved communication between stakeholders and private agricultural organizations, in order to mitigate the economic impacts of large yield losses of intensive crop farming. This may imply the adoption of crop insurances, the governmental expansion of trade investment funds to facilitate the international commercialization of agricultural products, and the diversification of regional sectors of activity to enhance local economies.

5. Conclusion

In this paper, we propose a methodology for mapping the global distribution of drought risk, based on the combination of independent indicators of historical drought hazard and current estimates of drought exposure and vulnerability. We concentrate on a top-down data driven approach that is consistent and suitable for all regions in the world. This map serves as a kind of first screening analysis to determine where local assessments of risk should be carried out to improve drought preparedness and strength appropriate drought management policies. We compute drought risk at the sub-national administrative level, thus allowing for better coordination and collaboration within and between different levels of government, from the local to the regional scales. The proposed model of drought risk is relative to the sample of geographic input regions and depends on the joint statistical distribution of the respective indicators of hazard, exposure and vulnerability. Therefore, the proposed scale of risk is not a measure of absolute losses or actual damage to human health or the environment, but suitable for ranking and comparison of input geographic regions.

Each determinant of drought risk is calculated independently of each other and based on indicators of different spatial resolutions. Drought hazard is computed globally at the 0.5°. This determinant of risk is derived from an analysis of historical sequences of monthly precipitation deficits for the period between 1901 and 2010. Drought exposure is computed at the sub-national level. It is based on a Data Envelopment Analysis (DEA) of very high spatial resolution gridded indicators of population and livestock density, crop cover and baseline water stress. Drought vulnerability is derived from the combination of high level factors of social, economic and infrastructural indicators, collected both at the national level and gridded layers of very high spatial resolution.

To validate the outcomes of the proposed approach, we implemented a performance evaluation of exposure and vulnerability models and assessed the spatial distribution of drought hazard and risk from the local to the regional scales. In detail, several alternative composite measures to the computation of drought exposure and vulnerability were formulated, computed and compared through internal validation criteria. Results indicate that the proposed models of exposure and vulnerability are more robust, consistent, and stable than alternative composite measures. Our findings support the idea that drought risk is driven by an exponential growth of regional exposure, while hazard and vulnerability exhibit a weaker relationship with the geographic distribution of risk values. Drought risk is lower for remote regions, such as tundras and tropical forests, and higher for populated areas and regions extensively exploited for crop production and livestock farming, such as South-Central Asia, Southeast of South America, Central Europe and Southeast of the United States. As climate change projections foresee an increase of drought frequency and intensity for currently exposed regions, then these results direct attention to aggravated risk for global food insecurity and potential for civil conflict. Nevertheless, as most agricultural regions show high infrastructural vulnerability, then regional drought risk management in these areas might benefit from an improvement of irrigation and water harvesting systems. From the economic viewpoint, reduction in drought risk may also be achieved by diversifying regional economies on different sectors of activity and reducing the dependence of their GDP on agriculture.

Finally, it is important to highlight that the proposed approach is fully data driven and the final results can be biased by the uncertainties of input indicators and propagation errors from their combination and aggregation. Although the quality of input proxy indicators can always be improved and regularly updated, we stress that the strength of our methodological approach is to build up a bridge between physical and social sciences to help policymakers to develop improved drought adaptation plans and establish drought mitigation activities. Nevertheless, we would like to direct attention to the fact that the top-down approach presented can complement but not replace detailed bottom-up risk studies for particular regions of interest.

References

Alcamo, J., Henrichs, T., 2002. Critical regions: a model-based estimation of world water resources sensitive to global changes. Aquat. Sci. 64, 352–362.
Alkire, S., Santos, M., 2014. Measuring acute poverty in the developing world: robustness and scope of the multidimensional poverty index. World Dev. 59, 251–274.
Alvarez-Buylla Roces, M.E., Lazos Chavero, E., García-Barrios, J.R., 1989. Homegardens of a humid tropical region in Southeast Mexico: an example of an agroforestry cropping system in a recently established community. Agroforest. Syst. 8, 133–156.
Anderson, G., Crawford, I., Leicester, A., 2011. Welfare rankings from multivariate data, a nonparametric approach. J. Public Econ. 95, 247–252.
Andrade, C., Belo-Pereira, M., 2015. Assessment of droughts in the Iberian Peninsula using the WASP-index. Atmos. Sci. Lett. 16, 208–218.
Arrow, K.J., 1951. Social Choice and Individual Values. Yale University Press.
Balk, D., Deichmann, U., Yetman, G., Pozzi, F., Hay, S., Nelson, A., 2006. Determining global population distribution: methods, applications and data. Adv. Parasitol. 62, 119–156.
Becker, A., Finger, P., Meyer-Christoffer, A., Rudolf, B., Schamm, K., Schneider, U., Ziese, M., 2013. A description of the global land-surface precipitation data products of the global precipitation climatology centre with sample applications including centennial (trend) analysis from 1901. Earth Syst. Sci. Data 5, 71–99.
Below, R., Grover-Kopec, E., Dilley, M., 2007. Documenting drought-related disasters: a global reassessment. J. Environ. Dev. 16, 328–344.
Blaikie, P., Cannon, T., Davis, I., Wisner, B., 1994. At Risk: Natural Hazards, People's Vulnerability and Disasters. Taylor & Francis.
Brasil-MI/MMA/MCT, 2005. Relatório Final do Grupo de Trabalho Interministerial para Redelimitaç ao do Semiárido Nordestino e do Polígono das Secas. Technical Report. Presidência da República, Brasília, Brasil.

Brasil-MMA, 2004. National action program to combat desertification and mitigate the effects of drought: PAN-Brazil, MMA Editions ISBN 85-87166-66-2. Environment Ministry, Water Resources Secretariat, Brasília, Brasil.

Brooks, N., Adger, W.N., Kelly, P.M., 2005. The determinants of vulnerability and adaptive capacity at the national level and the implications for adaptation. Glob. Environ. Change 15, 151–163.

Cardona, O., van Aalst, M., Birkmann, J., Fordham, M., McGregor, G., Perez, R., Pulwarty, R., Schipper, E., Sinh, B., 2012. Determinants of risk: exposure and vulnerability. In: Field, C., Barros, V., Stocker, T., Qin, D., Dokken, D., Ebi, K., Mastrandrea, M., Mach, K., Plattner, G.K., Allen, S., Tignor, M., Midgley, P. (Eds.), Managing the Risks of Extreme Events and Disasters to Advance Climate Change Adaptation. Cambridge University Press, pp. 65–108.

Carrão, H., Singleton, A., Naumann, G., Barbosa, P., Vogt, J., 2014. An optimized system for the classification of meteorological drought intensity with applications in frequency analysis. J. Appl. Meteorol. Climatol. 53, 1943–1960.

CEC, 2007. Impact Assessment. Accompanying document from the Commission to the European Parliament and the Council COM (207) Coordinating European Council, Brussels, Belgium.

Cook, W.D., Tone, K., Zhu, J., 2014. Data envelopment analysis: prior to choosing a model. Omega 44, 1–4.

Cook, W.D., 2006. Distance-based and ad hoc consensus models in ordinal preference ranking. Eur. J. Oper. Res. 172, 369–385.

Cooley, H., 2006. Floods and droughts. In: Gleick, P., Wolff, G., Cooley, H., Palaniappan, M., Samulon, A., Lee, E., Morrison, J., Katz, D. (Eds.), The World's Water 2006–2007: The Biennial Report on Freshwater Resources. Island Press, p. 392.

Cutter, S.L., Boruff, B.J., Shirley, W.L., 2003. Social vulnerability to environmental hazards. Soc. Sci. Q. 84, 242–261.

Dai, A., 2011. Drought under global warming: a review. Wiley Interdiscip. Rev. Clim. Change 2, 45–65.

Dao, H., Peduzzi, P., 2003. Global Risk And Vulnerability Index Trends per Year (GRAVITY). Technical annex and multiple risk integration Phase IV. UNDP/BCPR, Geneva.

Deichmann, U., Balk, D., Yetman, G., 2001. Transforming population data for interdisciplinary usages: From census to grid. Technical Report. NASA Socioeconomic Data and Applications Center (SEDAC), CIESIN. Columbia University, Palisades, NY.

Di Mauro, M., 2014. Quantifying risk before disasters occur: hazard information for probabilistic risk assessment. WMO Bull. 63, 36–41.

Dobson, J., Coleman, P., Durfee, R., Worley, B., 2000. Landscan: a global population database for estimating populations at risk. Photogramm. Eng. Remote Sens. 66, 849–857.

Downing, T., Bakker, K., 2000. Drought discourse and vulnerability. In: Wilhite, D.A. (Ed.), Drought: A Global Assessment, Natural Hazards and Disasters Series. Routledge Publishers, UK, pp. 213–230.

Dracup, J.A., Lee, K.S., Paulson Jr., E.G., 1980. On the definition of droughts. Water Resour. Res. 16, 297–302.

EEA, 2010. Mapping the impacts of natural hazards and technological accidents in Europe. An overview of the last decade. Technical Report 13/2010. European Environmental Agency, Copenhagen.

Eriyagama, N., Smakhtin, V., Gamage, N., 2009. Mapping drought patterns and impacts: a global perspective. Research report 133. International Water Management Institute (IWMI), Colombo, Sri Lanka.

FAO, 2014. Aquastat Database – Food and Agriculture Organization of the United Nations (FAO). Available online at http://www.fao.org/nr/water/aquastat/main/index.stm (cited 18.11.14).

FAO, 2015. The Global Administrative Unit Layers GAUL 2015 – Technical Aspects of the GAUL Distribution Set. Technical Report Doc01. Food and Agriculture Organization of the United Nations (FAO), Rome, Italy.

Güneralp, B., Güneralp, İ, Liu, Y., 2015. Changing global patterns of urban exposure to flood and drought hazards. Glob. Environ. Change 31, 217–225.

Gassert, F., Landis, M., Luck, M., Reig, P., Shiao, T., 2014. Aqueduct global maps 2.1. Working Paper. Available online at http://www.wri.org/publication/aqueduct-metadata-global.

Gassert, F., Luck, M., Landis, M., Reig, P., Shiao, T., 2014. Aqueduct global maps 2.1: Constructing decision-relevant global water risk indicators. Working Paper. Available online at http://www.wri.org/publication/aqueduct-globalmaps-21-indicators.

Getirana, A., 2016. Extreme water deficit in Brazil detected from space. J. Hydrometeorol. 17, 591–599.

Gleick, P.H., 2014. Water, drought, climate change, and conflict in Syria. Weather Clim. Soc. 6, 331–340.

Goddard, S., Harms, S.K., Reichenbach, S.E., Tadesse, T., Waltman, W.J., 2003. Geospatial decision support for drought risk management. Commun. ACM 46, 35–37.

González Tánago, I., Urquijo, J., Blauhut, V., Villarroya, F., De Stefano, L., 2015. Learning from experience: a systematic review of assessments of vulnerability to drought. Nat. Hazards 80, 951–973.

Gráda, C.Ó., 2007. Making famine history. J. Econ. Lit. 45, 5–38.

Gupta, S., Verhoeven, M., 2001. The efficiency of government expenditure: experiences from Africa. J. Policy Model. 23, 433–467.

Gupta, A.K., Tyagi, P., Sehgal, V.K., 2011. Drought disaster challenges and mitigation in India: strategic appraisal. Curr. Sci. 100, 1795–1806.

Hayes, M., Wilhelmi, O., Knutson, C., 2004. Reducing drought risk: bridging theory and practice. Nat. Hazards Rev. 5, 106–113.

He, B., Wu, J., Lü, A., Cui, X., Zhou, L., Liu, M., Zhao, L., 2012. Quantitative assessment and spatial characteristic analysis of agricultural drought risk in China. Nat. Hazards 66, 155–166.

Heim, R.R., 2002. A review of twentieth-century drought indices used in the United States. Bull. Am. Meteorol. Soc. 83, 1149–1165.

Heiser, W.J., D'Ambrosio, A., 2013. Clustering and prediction of rankings within a Kemeny distance framework. In: Lausen, B., den Poel, D.V., Ultsch, A. (Eds.), Algorithms From and for Nature and Life. Springer. Studies in Classification, Data Analysis, and Knowledge Organization, pp. 19–31.

Hernández, A.R.P., Martínez, L.R.B., Rueda, V.O.M., Matthias, A.D., Ruíz, J.J.L., 2008. Temporal and spatial behavior of temperature and precipitation during the canícula (midsummer drought) under el ni no conditions in Central México. Atmósfera 21, 265–280.

Hulme, M., 1996. Recent climatic change in the world's drylands. Geophys. Res. Lett. 23, 61–64.

Kallis, G., 2008. Droughts. Annu. Rev. Environ. Resour. 33, 85–118.

Kampragou, E., Apostolaki, S., Manoli, E., Froebrich, J., Assimacopoulos, D., 2011. Towards the harmonization of water-related policies for managing drought risks across the {EU}. Environ. Sci. Policy 14, 815–824.

Kelley, C.P., Mohtadi, S., Cane, M.A., Seager, R., Kushnir, Y., 2015. Climate change in the fertile crescent and implications of the recent Syrian drought. Proc. Natl. Acad. Sci. 112, 3241–3246.

Keyantash, J., Dracup, J.A., 2002. The quantification of drought: an evaluation of drought indices. Bull. Am. Meteorol. Soc. 83, 1167–1180.

Kim, H., Park, J., Yoo, J., Kim, T.W., 2015. Assessment of drought hazard, vulnerability, and risk: a case study for administrative districts in South Korea. J. Hydro-Environ. Res. 9, 28–35.

Lange, T., Roth, V., Braun, M.L., Buhmann, J.M., 2004. Stability-based validation of clustering solutions. Neural Comput. 16.

Lavell, A., 1994. Prevention and mitigation of disasters in Central America: vulnerability to disasters at the local level. In: Varley, A. (Ed.), Disasters, Development, and Environment. Wiley, New York, pp. 49–63.

Llano, M.P., Vargas, W., Naumann, G., 2012. Climate variability in areas of the world with high production of soya beans and corn: its relationship to crop yields. Meteorol. Appl. 19, 385–396.

Lovell, C., Pastor, J.T., 1999. Radial {DEA} models without inputs or without outputs. Eur. J. Oper. Res. 118, 46–51.

Lyon, B., Barnston, A.G., 2005. ENSO and the spatial extent of interannual precipitation extremes in tropical land areas. J. Clim. 18, 5095–5109.

Magrin, G., García, C.G., Choque, D.C., Giménez, J.C., Moreno, A.R., Nagy, G.J., Nobre, C., Villamizar, A., 2007. Climate change 2007: impacts, adaptation and vulnerability. In: Parry, M.L., Canziani, O.F., Palutikof, J.P., van der Linden, P.J., Hanson, C.E. (Eds.), Contribution of Working Group II to the Fourth Assessment Report of the Intergovernmental Panel on Climate Change. Cambridge University Press, pp. 581–615.

Masutomi, Y., Inui, Y., Takahashi, K., Matsuoka, Y., 2009. Development of highly accurate global polygonal drainage basin data. Hydrol. Process. 23, 572–584.

Mishra, A.K., Singh, V.P., 2009. A review of drought concepts. J. Hydrol. 391, 202–216.

Mishra, A.K., Singh, V.P., Desai, V.R., 2009. Drought characterization: a probabilistic approach. Stoch. Environ. Res. Risk Assess. 23, 41–45.

Naumann, G., Barbosa, P., Garrote, L., Iglesias, A., Vogt, J., 2014. Exploring drought vulnerability in Africa: an indicator based analysis to be used in early warning systems. Hydrol. Earth Syst. Sci. 18, 1591–1604.

NCDC, 2015. Billion-Dollar Weather and Climate Disasters: Overview. Available online at http://www.ncdc.noaa.gov/billions/overview.

OECD/JRC, 2008. Handbook on Constructing Composite Indicators. Methodology and User Guide. Social Policies and Data Series. OECD Publisher, Paris.

Parré, J.L., Guilhoto, J.J.M., 2001. A desconcentrac ao regional do agronegocio brasileiro. Rev. Bras. Econ. 55, 223–251.

Peduzzi, P., Dao, H., Herold, C., Mouton, F., 2009. Assessing global exposure and vulnerability towards natural hazards: the disaster risk index. Nat. Hazards Earth Syst. Sci. 9, 1149–1159.

Peterson, T.C., Hoerling, M.P., Stott, P.A., Herring, S.C., 2013. Explaining extreme events of 2012 from a climate perspective. Bull. Am. Meteorol. Soc. 94, S1–S74.

Pielke, R., Rubiera, J., Landsea, C., Fernndez, M., Klein, R., 2003. Hurricane vulnerability in Latin America and the Caribbean. Normalized damage and loss potentials. Nat. Hazard. Rev. 4, 101–114.

Pozzi, W., Sheffield, J., Stefanski, R., Cripe, D., Pulwarty, R., Vogt Jr., J.V.R.R.H., Brewer, M.J., Svoboda, M., Westerhoff, R., van Dijk, A.I.J.M., Lloyd-Hughes, B., Pappenberger, F., Werner, M., Dutra, E., Wetterhall, F., Wagner, W., Schubert, S., Mo, K., Nicholson, M., Bettio, L., Nunez, L., van Beek, R., Bierkens, M., de Goncalves, L.G.G., de Mattos, J.G.Z., Lawford, R., 2013. Toward global drought early warning capability: expanding international cooperation for the development of a framework for monitoring and forecasting. Bull. Am. Meteorol. Soc. 94, 776–785.

Pulwarty, R.S., Sivakumar, M.V., 2014. Information systems in a changing climate: early warnings and drought risk management. Weather Clim. Extremes 3, 14–21.

Ramankutty, N., Evan, A.T., Monfreda, C., Foley, J.A., 2008. Farming the planet: 1. Geographic distribution of global agricultural lands in the year 2000. Glob. Biogeochem. Cycles 22,, n/a–n/a.

Ramos, X., Silber, J., 2005. On the application of efficiency analysis to the study of the dimensions of human development. Rev. Income Wealth 51, 285–309.

Reed, S., 1997. Crop Adaptation to Climate Change. UNDP/UNDRO Disaster Management Training Programme, 3rd ed..

Robinson, T.P., Wint, G.R.W., Conchedda, G., Van Boeckel, T.P., Ercoli, V., Palamara, E., Cinardi, G., D'Aietti, L., Hay, S.I., Gilbert, M., 2014. Mapping the global distribution of livestock. PLOS ONE 9, e96084.

Rodríguez, O.P., Alocn, J.C., Elvir, C.Z., 2012. Buenas prácticas para la seguridad alimentaria y la gestión de riesgo. Acción contra el Hambre (ACF) 19627. Organización de las Naciones Unidas para la Alimentación y la Agricultura (FAO), Tegucigalpa, Honduras.

Russo, S., Dosio, A., Sterl, A., Barbosa, P., Vogt, J., 2013. Projection of occurrence of extreme dry-wet years and seasons in Europe with stationary and nonstationary standardized precipitation indices. J. Geophys. Res. D: Atmos. 118.

Scoones, I., 1998. Sustainable Rural Livelihoods: A Framework for Analysis. Working Paper 72. Institute of Development Studies (IDS), Brighton.

Seager, R., Ting, M., Held, I., Kushnir, Y., Lu, J., Vecchi, G., Huang, H.P., Harnik, N., Leetmaa, A., Lau, N.C., Li, C., Velez, J., Naik, N., 2007. Model projections of an imminent transition to a more arid climate in Southwestern North America. Science 316, 1181–1184.

Shahid, S., Behrawan, H., 2008. Drought risk assessment in the western part of Bangladesh. Nat. Hazards 46, 391–413.

Shiau, J.T., Hsiao, Y.Y., 2012. Water-deficit-based drought risk assessments in Taiwan. Nat. Hazards 64, 237–257.

Sivakumar, M.V., Stefanski, R., Bazza, M., Zelaya, S., Wilhite, D., Magalhaes, A.R., 2014. High level meeting on national drought policy: summary and major outcomes. Weather Clim. Extremes 3, 126–132.

Spinoni, J., Naumann, G., Carrão, H., Barbosa, P., Vogt, J., 2014. World drought frequency, duration, and severity for 1951–2010. Int. J. Climatol. 34, 2792–2804.

Spinoni, J., Vogt, J., Naumann, G., Carrão, H., Barbosa, P., 2015. Towards identifying areas at climatological risk of desertification using the köppengeiger classification and fao aridity index. Int. J. Climatol. 35, 2210–2222.

Svoboda, M., Hayes, M., Wood, D., 2012. Standardized Precipitation Index User Guide. Technical Report WMO-No. 1090. World Meteorological Organization (WMO), Geneva.

Svoboda, M.D., Fuchs, B.A., Poulsen, C.C., Nothwehr, J.R., 2015. The drought risk atlas: enhancing decision support for drought risk management in the United States. J. Hydrol. 526, 274–286.

Tobler, W., Deichmann, U., Gottsegen, J., Maloy, K., 1997. World population in a grid of spherical quadrilaterals. Int. J. Popul. Geogr. 3, 203–225.

Traore, S.B., Ali, A., Tinni, S.H., Samake, M., Garba, I., Maigari, I., Alhassane, A., Samba, A., Diao, M.B., Atta, S., Dieye, P.O., Nacro, H.B., Bouafou, K.G., 2014. Agrhymet: a drought monitoring and capacity building center in the West Africa region. Weather Clim. Extremes 3, 22–30.

Trenberth, K.E., Stepaniak, D., 2011. Indices of el Ni no evolution. J. Clim. 14, 1697–1701.

UN-DESA, 2013. Establishing Drought Early Warning Systems in West Asia and North Africa. Technical Report. United Nations Department of Economic and Social Affairs, New York, USA.

UNDP, 2013. The Rise of the South: Human Progress in a Diverse World. Human Development Reports 1990–2013 23. United Nations Development Programme, New York, USA.

UNISDR, 2004. Living with Risk: A Global Review of Disaster Reduction Initiatives. Review Volume 1. United Nations International Strategy for Disaster Reduction, Geneva, Switzerland.

UNISDR, 2009a. Drought Risk Reduction Framework and Practices: Contributing to the Implementation of the Hyogo Framework for Action. Technical Report. United Nations International Strategy for Disaster Reduction, Geneva, Switzerland.

UNISDR, 2009b. Global assessment report on disaster risk reduction. Technical Report. United Nations International Strategy for Disaster Reduction, Geneva, Switzerland.

van der Zee Arias, A., van der Zee, J., Meyrat, A., Poveda, C., Picado, L., 2012. Estudio de la caracterización del Corredor Seco Centroamericano. Acción contra el Hambre (ACF) Pases CA-4. Organización de las Naciones Unidas para la Alimentación y la Agricultura (FAO), Tegucigalpa, Honduras.

van der Zee Arias, A., van der Zee, J., Meyrat, A., Poveda, C., Picado, L., 2012. Identificación de Actores Relevantes y relaciones interistitucionales en el Corredor Seco Centroamericano. Acción contra el Hambre (ACF) Pases CA-4. Organización de las Naciones Unidas para la Alimentación y la Agricultura (FAO), Tegucigalpa, Honduras.

Van Loon, A.F., Van Lanen, H.A.J., 2013. Making the distinction between water scarcity and drought using an observation-modeling framework. Water Resour. Res. 49, 1483–1502.

Wilhite, D., Buchanan, M., 2005. Drought as hazard: understanding the natural and social context. In: Wilhite, D.A. (Ed.), Drought and Water Crisis: Science, Technology, and Management Issues. CRC Press (Taylor and Francis), New York, pp. 3–29.

Wilhite, D.A., Glantz, M.H., 1985. Understanding the drought phenomenon. The role of definitions. Water Int. 10, 111–120.

Wilhite, D.A., Pulwarty, R.S., 2005. Lessons learned and the road ahead. In: Wilhite, D.A. (Ed.), Drought and Water Crisis: Science, Technology, and Management Issues. CRC Press (Taylor and Francis), New York, pp. 389–398.

Wilhite, D.A., Svoboda, M.D., Hayes, M.J., 2007. Understanding the complex impacts of drought: a key to enhancing drought mitigation and preparedness. Water Resour. Manag. 21, 763–774.

Wilhite, D.A., Sivakumar, M.V., Pulwarty, R., 2014. Managing drought risk in a changing climate: the role of national drought policy. Weather Clim. Extremes 3, 4–13.

Wilhite, D., 2000. Drought as a natural hazard: concepts and definitions. In: Wilhite, D.A. (Ed.), Drought: A Global Assessment, Natural Hazards and Disasters Series. Routledge Publishers, UK, pp. 213–230.

WMO, 2013. High-level Meeting on National Drought Policy. Meeting Minutes. World Meteorological Organization, Geneva, Switzerland.

Yadav, S., Redden, R., Hatfield, J., Lotze-Campen, H., Hall, A., 2011. Crop Adaptation to Climate Change. Wiley.